# Optimal Mass Transport for Medical Image Computation

**Allen Tannenbaum**
**Computer Science and Applied Mathematics/Statistics**
**Stony Brook University**

**http://www.na-mic.org/Wiki/index.php/Algorithm:BU**

In collaboration with (no particular order):

Sigurd Angenent
Steven Haker
Eldad Haber
Tauseef ur-Rehman
Tryphon Georgiou
Emmanuel Tannenbaum
Ayelet Dominitz
Guillermo Sapiro
Eric Pichon
Ron Kikinis
Delphine Nain

Tony Yezzi
Wilfrid Gangbo
Wassim Haddad
Behnood Gholami
Marc Niethammer
Oleg Michaelovich
Namrata Vaswami
Peter Karasev
Steven Zucker
Arie Nakhmani
Yogesh Rathi
Patricio Vela

# Medical Applications: IGT and IGS

- Biomedical engineering/applied mathematical principles to develop general-purpose algorithms and software that can be integrated into complete therapy/surgical  delivery systems.

- Four main components of image-guided therapy (IGT): localization, targeting, monitoring and control.

- Develop robust algorithms for:
  - Segmentation - automated methods that create patient-specific models of relevant anatomy from multi-modal data.
  - Registration – automated methods that align multiple data sets with each other and with the patient.

# Advanced Multimodality Image-Guided Operating (AMIGO) Suite

The AMIGO Suite is the nation's first integrated operating suite to offer immediate intra-procedural access to an extensive range of advanced imaging modalities. AMIGO's 5,700 square-foot space is divided into three interconnected procedure rooms housing real-time anatomic, functional, and molecular imaging, including 3T MRI, PET/CT, fluoroscopy, and ultrasound.

- Image Processing, Dynamics, and Control
- Evolving Shapes Statically and Dynamically
- Statistics, Shape, and Estimation
- Interactive Methods

# Shapes

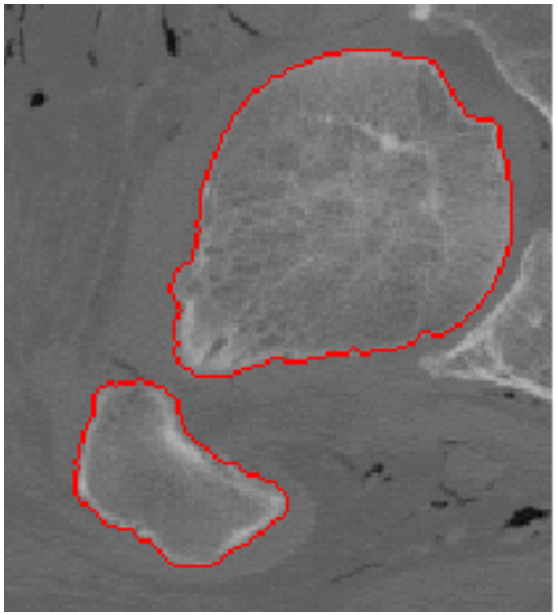

Closed curve

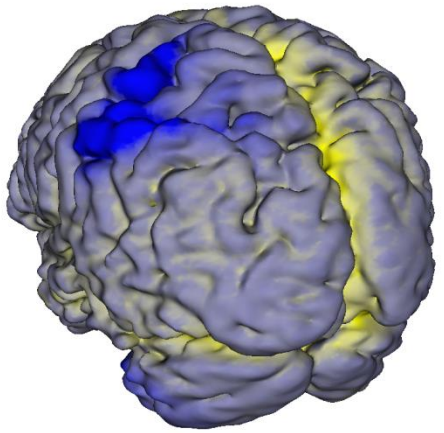

Closed surface

# Classical Image Processing

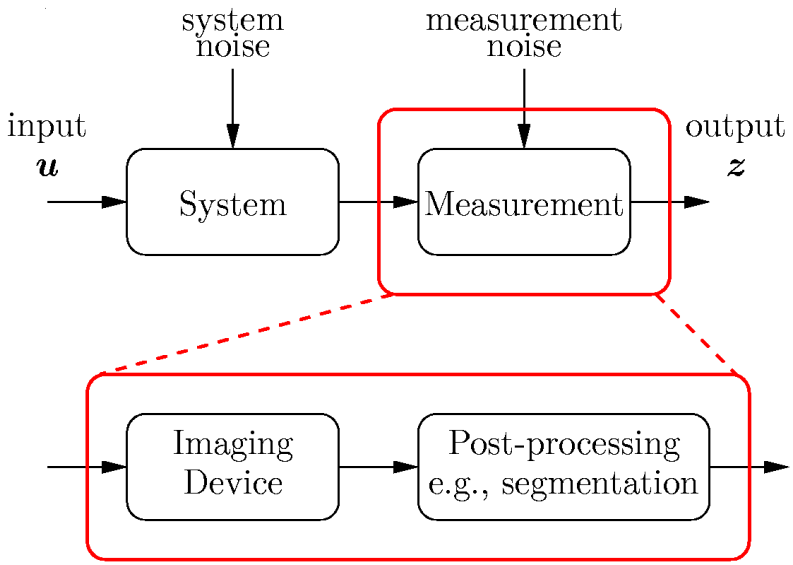


System:

plane, brain, heart, ...

Measurement:

imaging + post-processing, camera, fMRI, MRI, ...

What happens if measurements change over time?

How to influence the system by measured output?

“How to combine image processing, control, and machine learning for medical image computation?”

# Examples of Shape Variation

Multiple patients

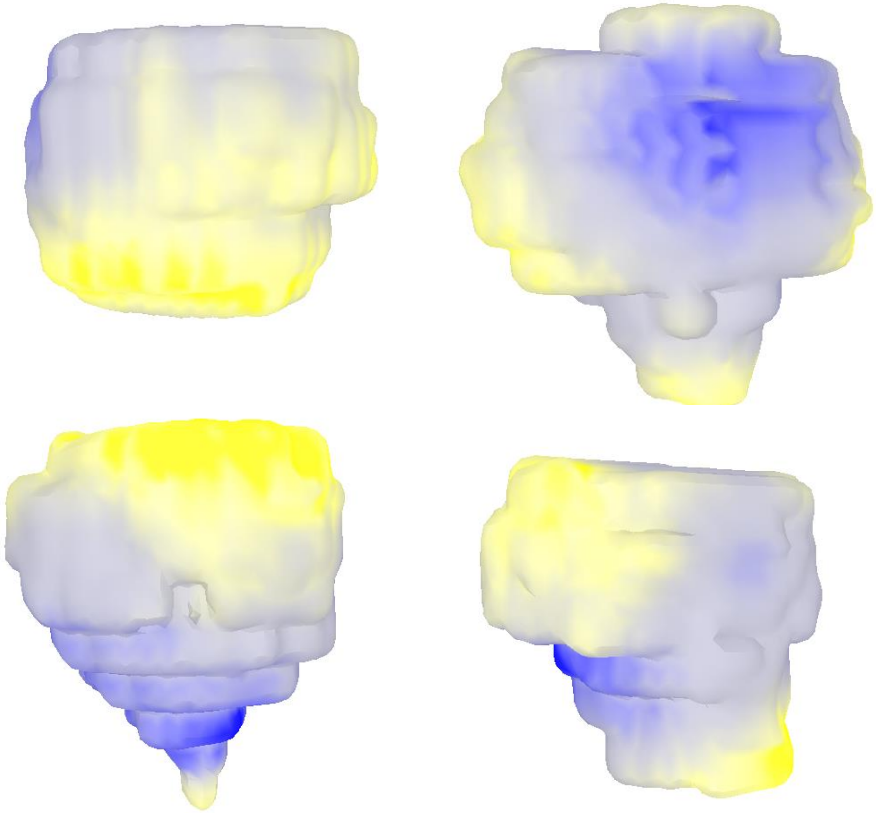

Temporal

[Dataset from C. Tempany MD, A. Szot MD, J. Zhang MD, S. Haker Ph.D.]

# Surface Deformations and Flattening

- Conformal and Area-Preserving Maps
  - Optical Flow
- Gives Parametrization of Surface
  - Registration
- Shows Details Hidden in Surface Folds
- Path Planning
  - Fly-Throughs
- Medical Research
  - Brain, Colon, Bronchial Pathologies
  - Functional MR and Neural Activity
- Computer Graphics and Visualization
  - Texture Mapping

# Mathematical Theory of Surface Mapping

- Conformal Mapping:
  - One-one
  - Angle Preserving
  - Fundamental Form

$$(E, F, G) \rightarrow \rho(E, F, G)$$

- Examples of Conformal Mappings:
  - One-one Holomorphic Functions
  - Spherical Projection

- Uniformization Theorem:
  - Existence of Conformal Mappings
  - Uniqueness of Mapping

# Deriving the Mapping Equation

Let $p$ be a point on the surface $\Sigma$. Let

$$z : \Sigma \rightarrow S^2$$

be a conformal equivalence sending $p$ to the North Pole.

Introduce **Conformal Coordinates** $(u, v)$ near $p$, with $u = v = 0$ at $p$.

In these coordinates, $ds^2 = \lambda(u,v)^2 \left( du^2 + dv^2 \right)$

We can ensure that $\lambda(p) = 1$.

In these coordinates, the Laplace Beltrami operator takes the form

$$\Delta = \frac{1}{\lambda(u,v)^2} \left( \frac{\partial^2}{\partial u^2} + \frac{\partial^2}{\partial v^2} \right).$$

# Deriving the Equation-Continued

Set $w = u + iv$. The mapping $z = z(w)$ has a simple pole at $w = 0$, i.e. at $p$ .

Near $p$ , we have a Laurent series $z(w) = \frac{A}{w} + B + C + Dw^2 + \ldots$

Apply $\Delta$ to get $\Delta z = A\Delta\left(\frac{1}{w}\right)$.

Taking $A = \frac{1}{2\pi}$,

$$\begin{aligned}
\Delta z &= \frac{1}{2\pi}\Delta\left(\frac{1}{w}\right) \\
&= \frac{1}{2\pi}\Delta\left(\frac{\partial}{\partial u} - i\frac{\partial}{\partial v}\right)\log|w| \\
&= \frac{1}{2\pi}\left(\frac{\partial}{\partial u} - i\frac{\partial}{\partial v}\right)\Delta\log|w| \\
&= \frac{1}{2\pi}\left(\frac{\partial}{\partial u} - i\frac{\partial}{\partial v}\right)(2\,\pi\,\delta_p)
\end{aligned}$$

# The Mapping Equation

$$\Delta z = \left( \frac{\partial}{\partial u} - i \frac{\partial}{\partial v} \right) \delta_p .$$

**Simply a second order linear PDE. Solvable by standard methods**.

# Cortical Surface Flattening-Normal Brain

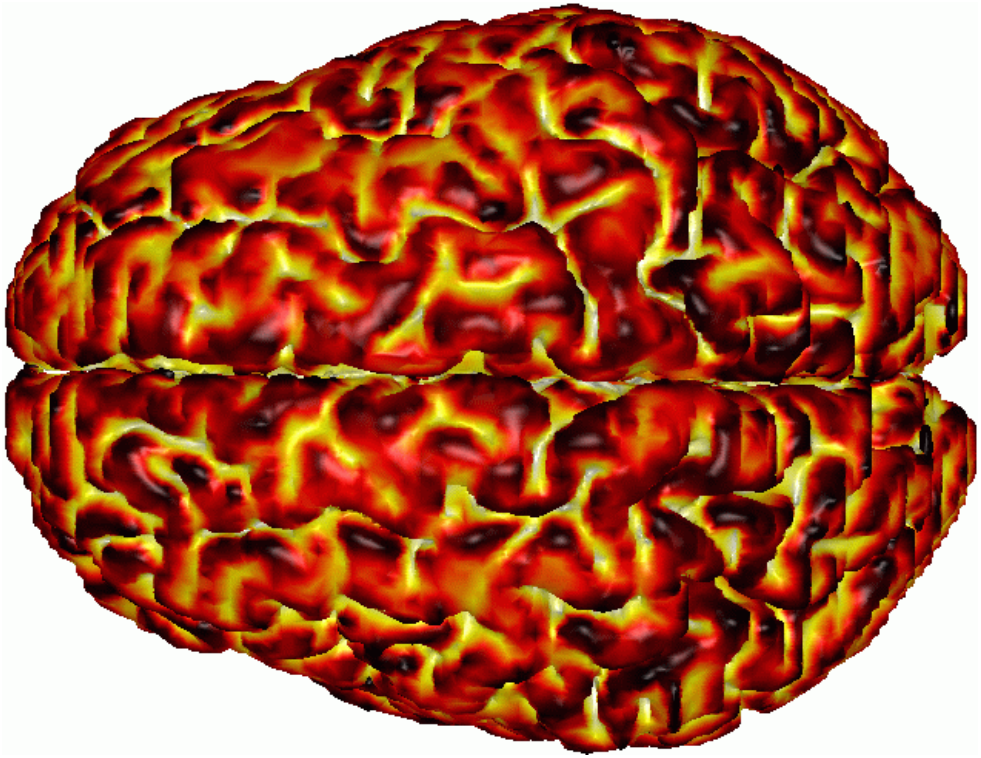

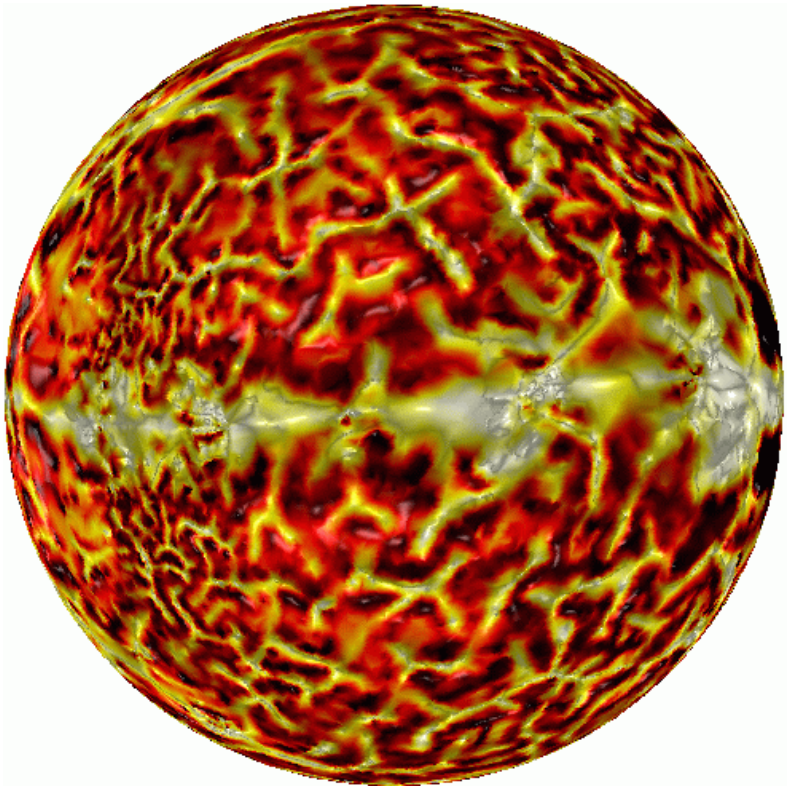

# White Matter Segmentation and Flattening

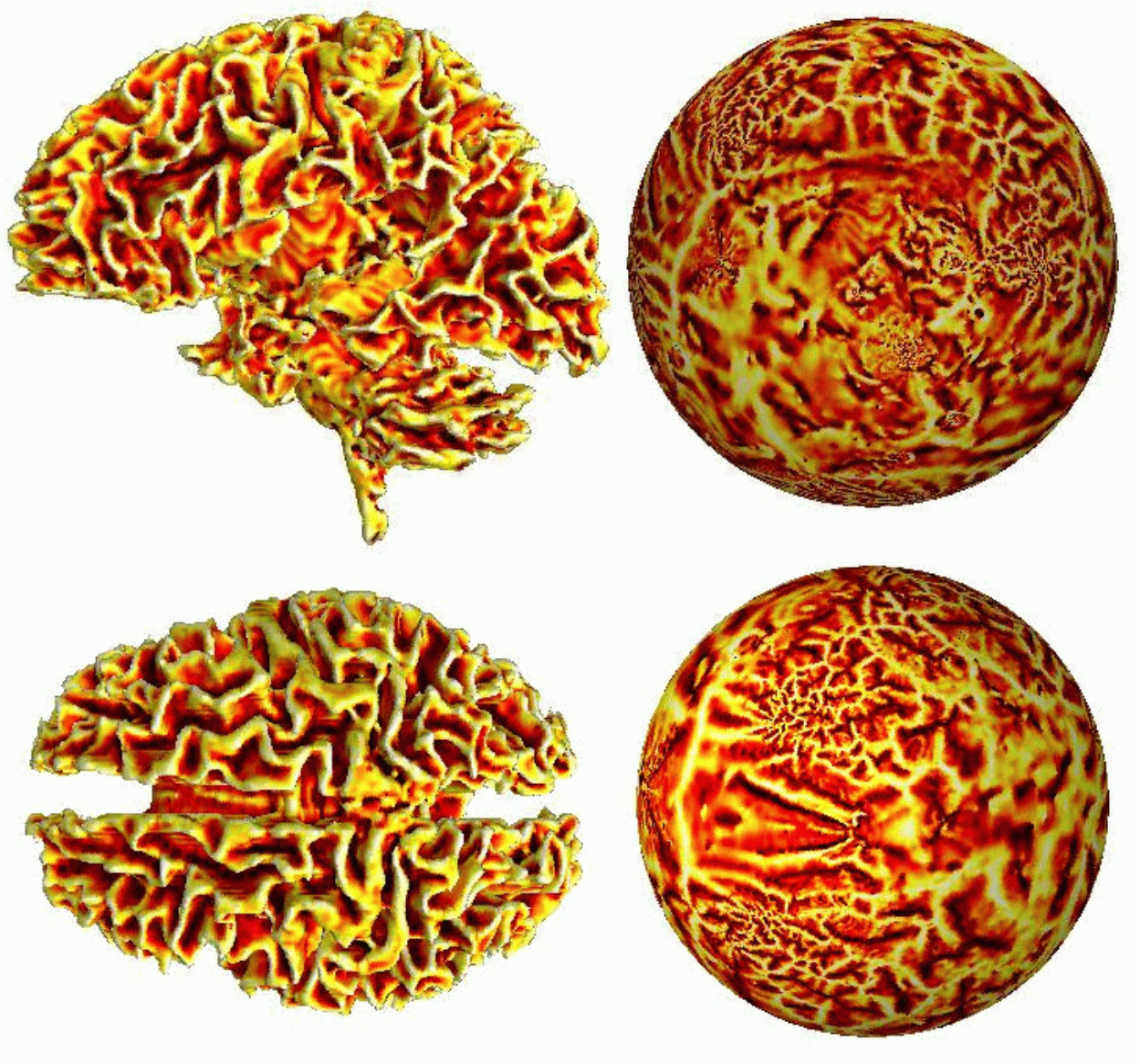

# Conformal Mapping of Neonate Cortex

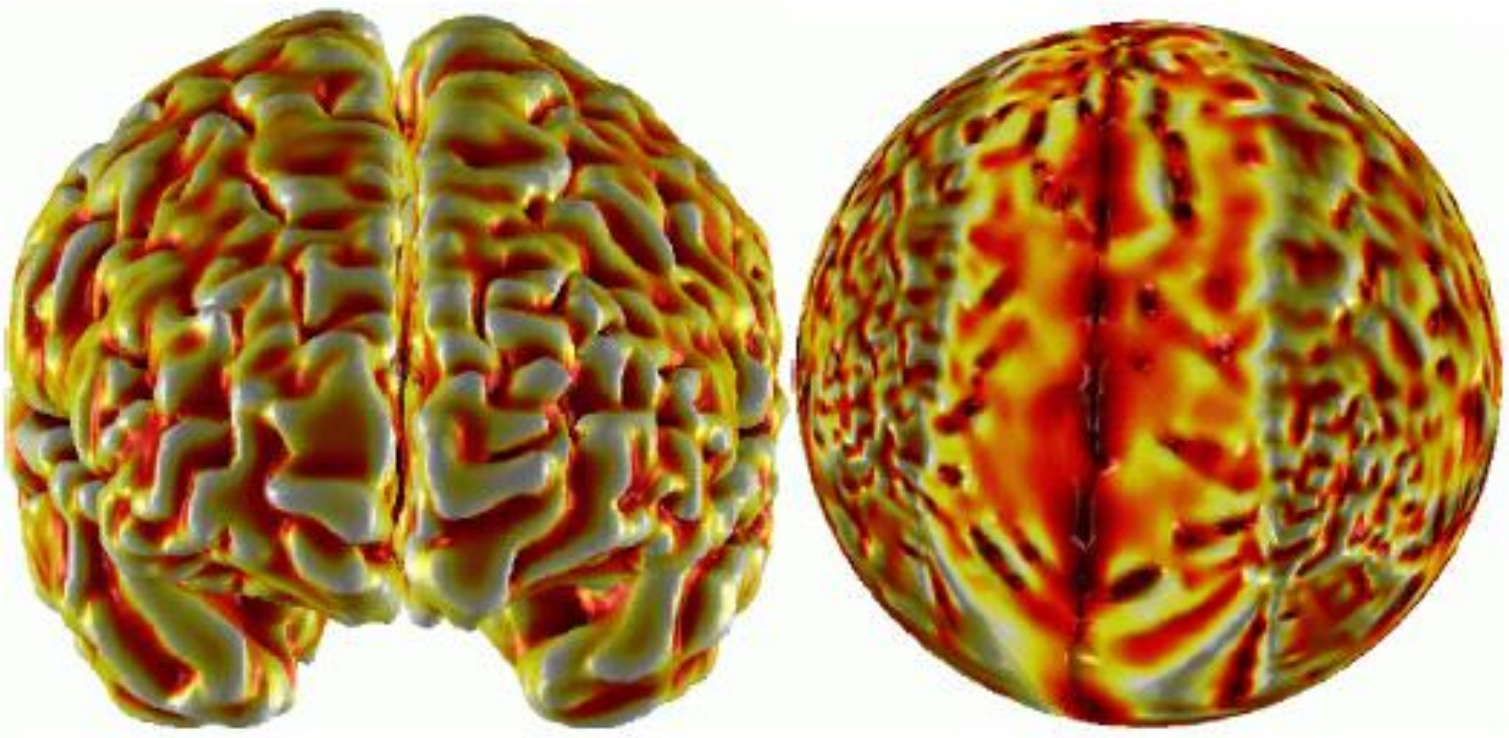

**Figure 8.4.5-12**
Conformal mapping of the neonate cortical surface to the sphere. The shading scheme represents mean curvature.

# Flattening a Tube

**(1) Solve**

$$\Delta u = 0 \ \text{ on } \Sigma \setminus (\sigma_0 \cup \sigma_1)$$

$$u = 0 \ \text{ on } \ \sigma_0$$

$$u = 1 \ \text{ on } \ \sigma_1$$

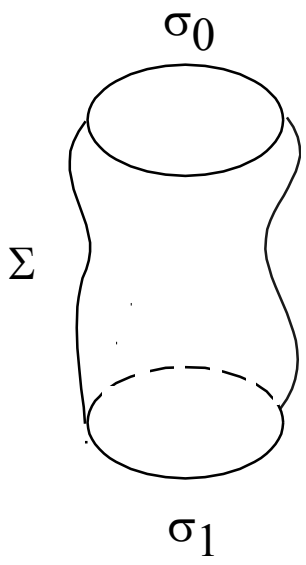


**(2) Make a cut from $\sigma_0$ to $\sigma_1$ .**

**Make sure $u$ is increasing along the cut.**

# Flattening a Tube-Continued

**(3) Calculate** $v$ **on the boundary loop**

$$\sigma_0 \to cut \to \sigma_1 \to cut \to \sigma_0$$

**by integration**

$$v(\xi) = \int^{\xi} \frac{\partial v}{\partial s} ds = \int^{\xi} \frac{\partial u}{\partial n} ds$$

**(4) Solve Dirichlet problem using boundary values of** $v$ **.**

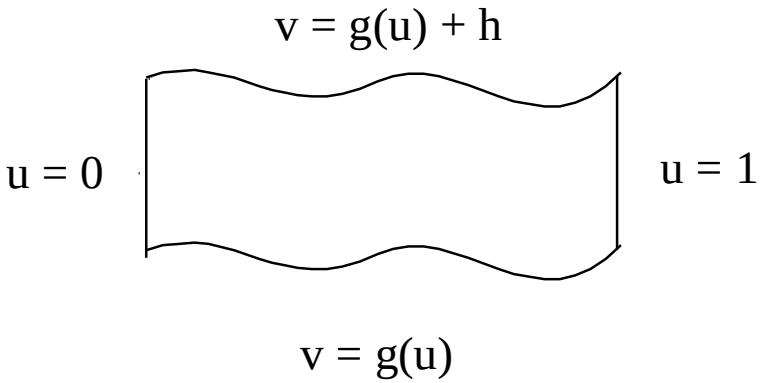


**If you want, scale so** $h = 2\pi$**, take** $e^{u+iv}$ **to get an annulus.**

# Flattening Without Distortion-I

**In practice, once the tubular surface has been flattened into a rectangular shape, it will need to be visually inspected for pathologies. We present a simple technique by which the entire colon surface can be presented to the viewer as a sequence of images or cine. In addition, this method allows the viewer to examine each surface point without distortion at some time in the cine. Here, we will say a mapping is without distortion at a point if it preserves the intrinsic distance there.**

**It is well known that a surface cannot in general be flattened onto the plane without some distortion somewhere. However, it may be possible to achieve a surface flattening which is free of distortion along some curve. A simple example of this is the familiar Mercator projection of the earth, in which the equator appears without distortion. In our case, the distortion free curve will be a level set of the harmonic function (essentially a loop around the tubular colon surface), and will correspond to the vertical line through the center of a frame in the cine. This line is orthogonal to the "path of flight" so that every point of the colon surface is exhibited at some time without distortion.**

# Flattening Without Distortion-II

Suppose we have conformally flattened the colon surface onto a rectangle

$$R = [0, u_{\max}] \times [-\pi, \pi].$$

Let $F$ be the inverse of this mapping, and let $\phi^2 = \phi^2(u,v)$ be the amount by Which $F$ scales a small area near $(u,v)$, i.e. let $\phi > 0$ be the "conformal factor" for $F$.

Fix $w > 0$, and for each $u_0 \in [0, u_{\max}]$ define a subset $R_0 = ([u_0 - w, u_0 + w] \times [-\pi, \pi]) \cap R$ which will correspond to the contents of a cine frame. We define a mapping

$$(\hat{u}, \hat{v}) = G(u,v) = \left( \int_{u_0}^{u} \phi(\mu, v) d\mu, \int_{0}^{v} \phi(u_0, v) dv \right).$$

# Flattening Without Distortion-III

We have

$$dG(u,v)=\begin{pmatrix}\hat{u}_u & \hat{u}_v\\ \hat{v}_u & \hat{v}_v\end{pmatrix}=\begin{pmatrix}\phi(u,v) & \int_{u_0}^{u}\phi_v(\mu,v)d\mu\\ 0 & \phi(u_0,v)\end{pmatrix},$$

$$dG(u_0,v)=\phi(u_0,v)\times\begin{pmatrix}1 & 0\\ 0 & 1\end{pmatrix}.$$

This implies that composition of the flattening map with $G$ sends level set loop $\{u=u_0\}$ on the surface to the vertical line $\{\hat{u}=0\}$ in the $\hat{u}-\hat{v}$ plane without distortion. In addition, it follows from the formula for $dG$ that lengths measured in the $\hat{u}$ direction accurately reflect the lengths of corresponding curves on the surface.

# Problems of CT Colonography

- Proper preparation of bowel
- How to ensure complete inspection

→ Nondistorting colon flattening program

# Nondistorting colon flattening

- Simulating pathologist’ approach
- No Navigation is needed
- Entire surface is visualized

# Nondistorting Colon Flattening

- Using CT colonography data
- Standard protocol for CT colonography
- Sixty-three patients (38 m, 25 f)
- Mean age 70.2 years (from 50 to 82)

# Flattened Colon

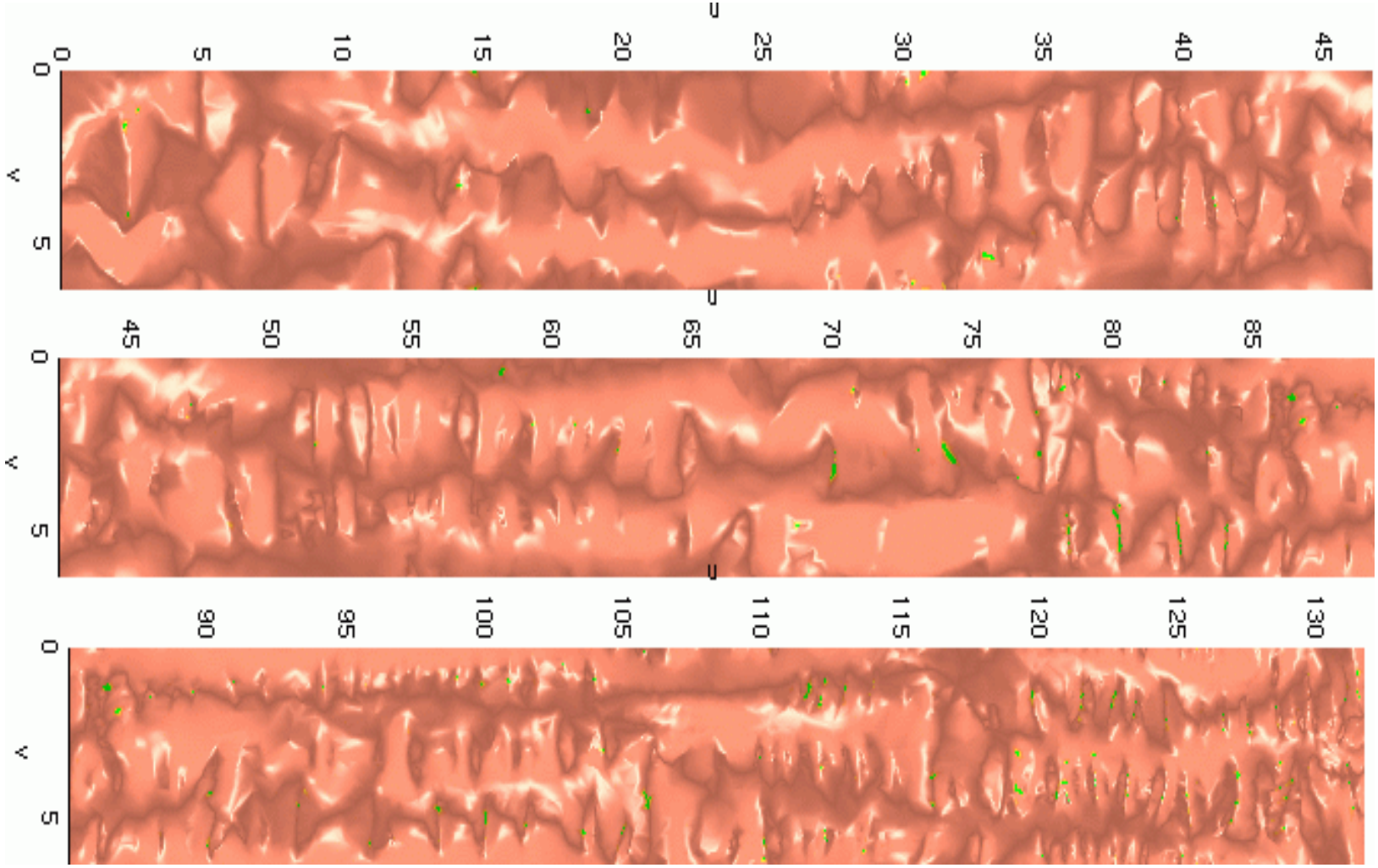

# Polyps Rendering

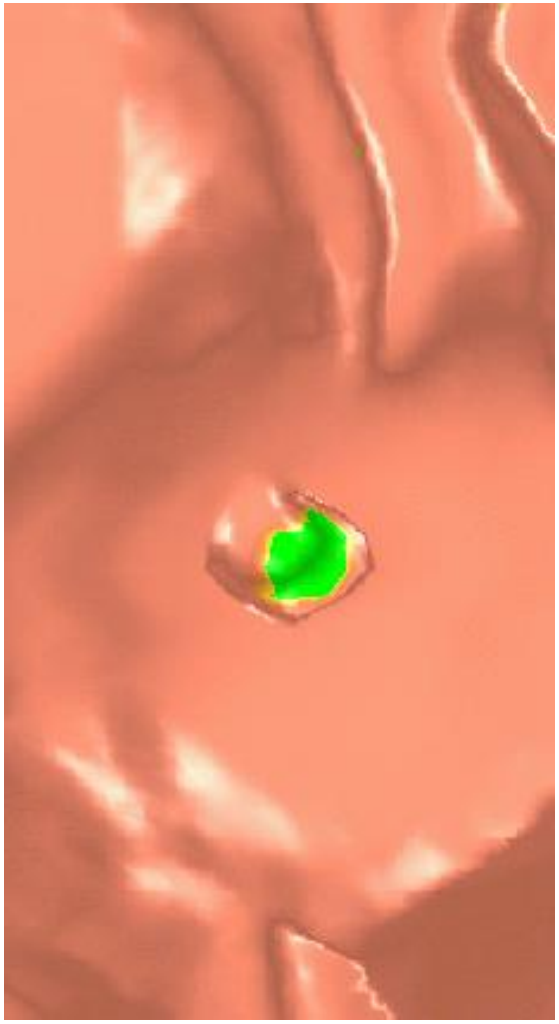

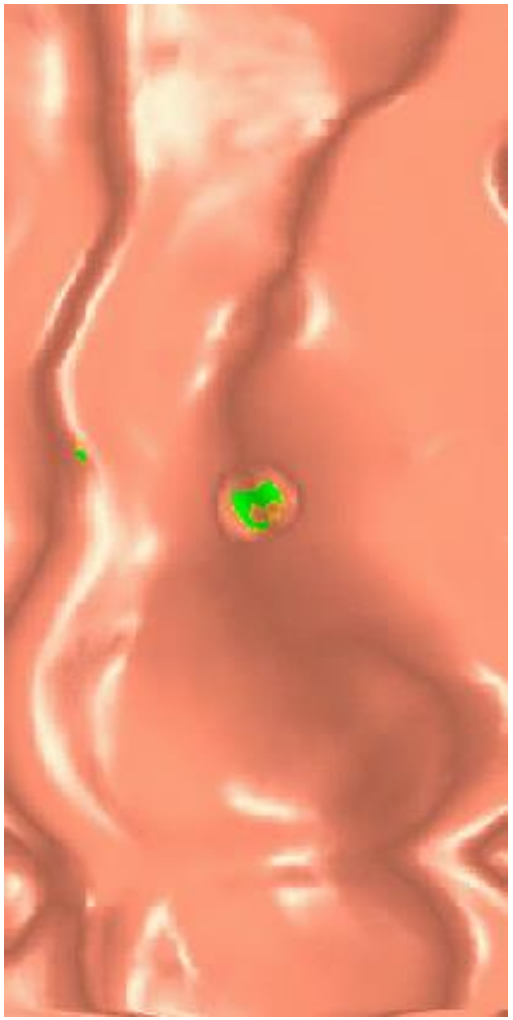

# Finding Polyps on Original Images

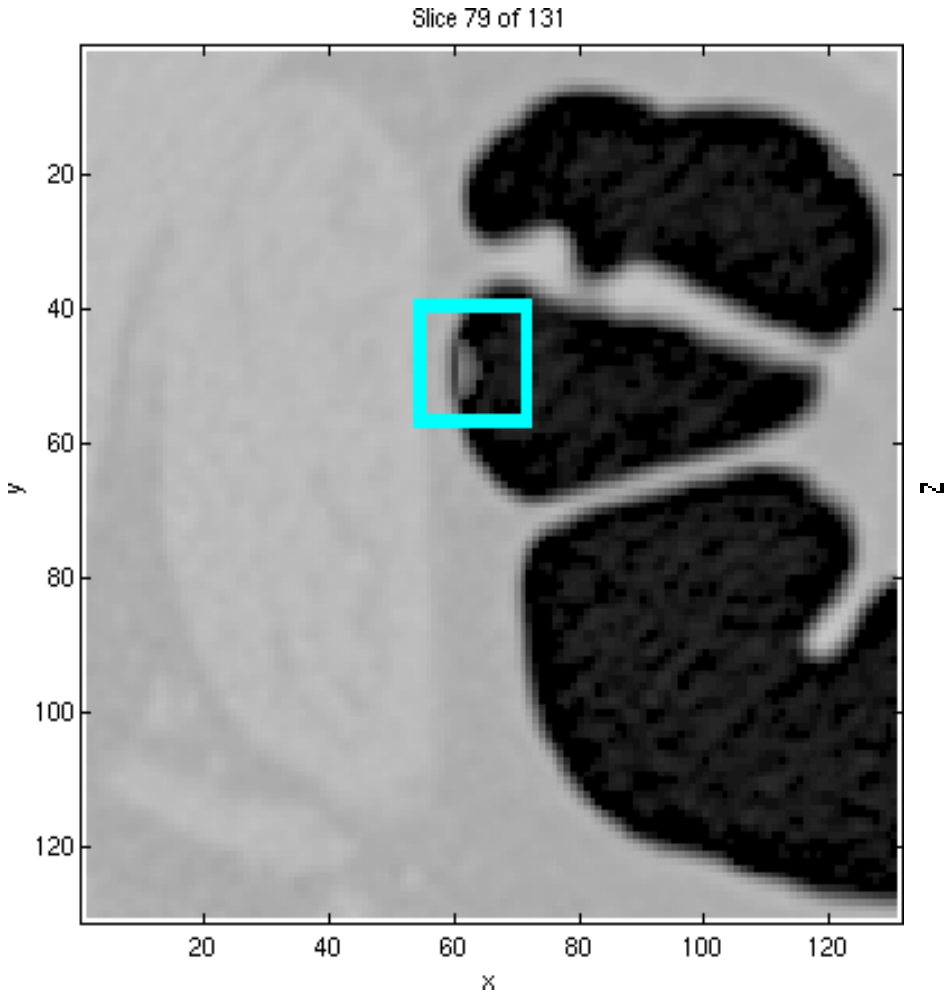


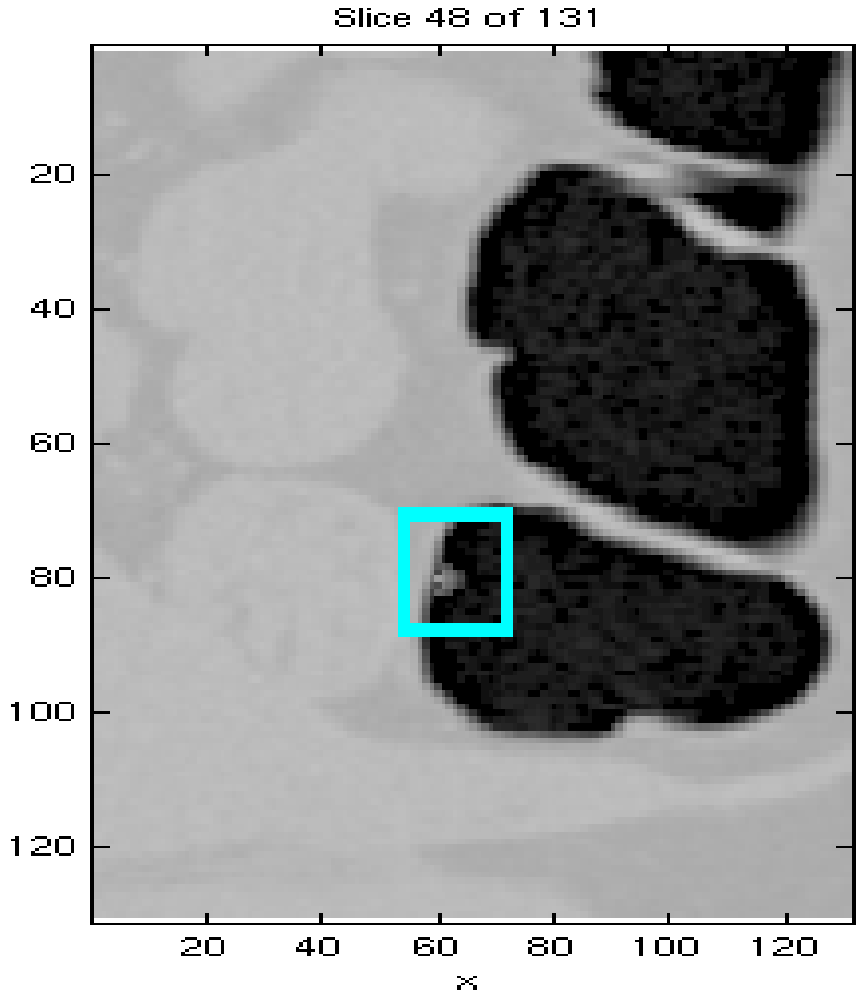

# Colon Fly-Through

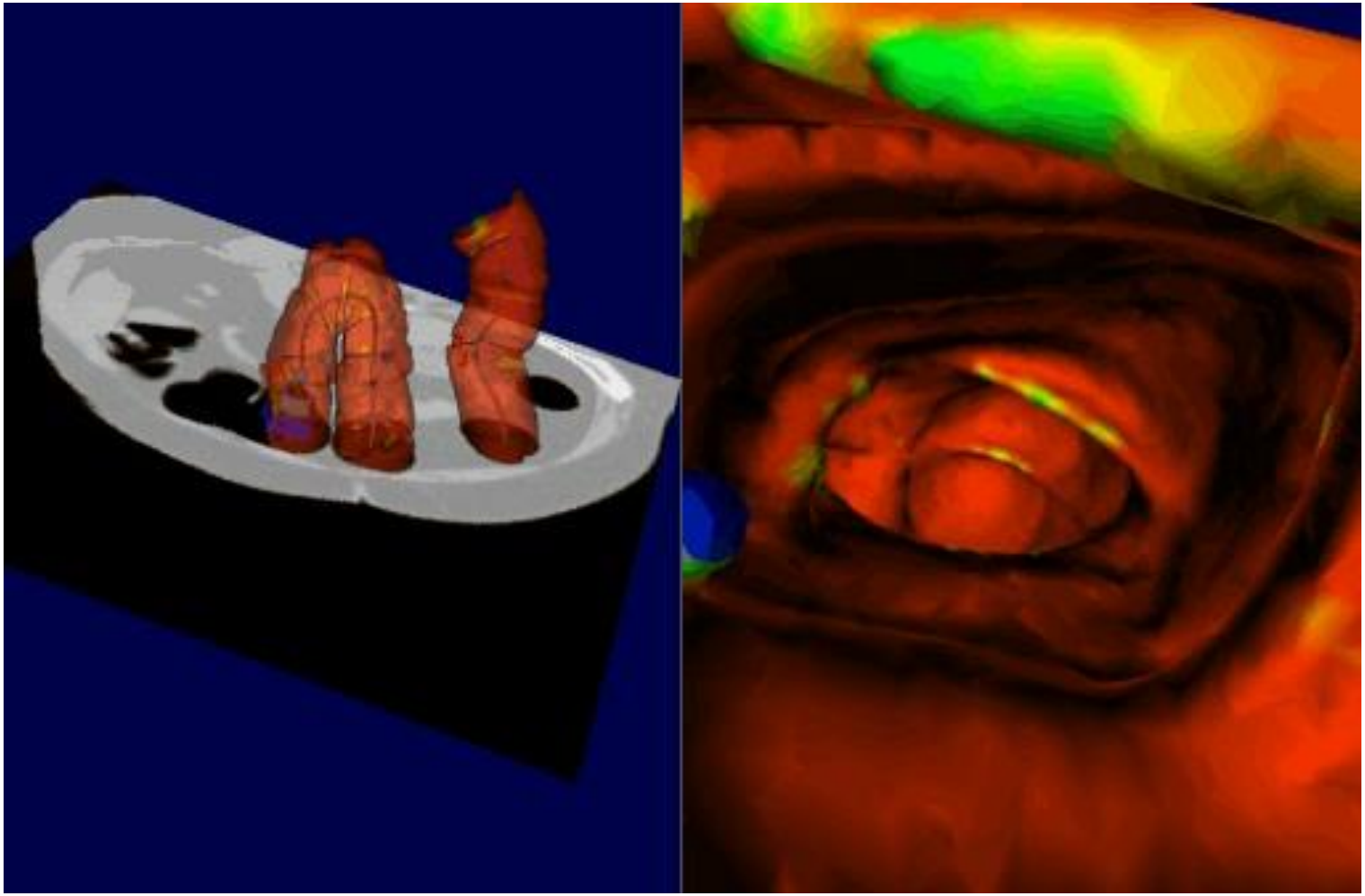

# Area-Preserving Flows-I

Let M be a closed, connected n-dimensional manifold. **Volume form:**

$$\tau = g(x)\,dx\,,\ dx = dx_1 \wedge \ldots \wedge dx_n,$$
$$g(x) > 0$$

**Theorem (Moser):**

M, N compact manifolds with volume forms $\tau$ and $\sigma$. Assume that M and N are diffeomorphic. If

$$\int_M \tau = \int_N \sigma,$$

then there exists a diffeomorphism of M into N taking $\tau$ into $\sigma$.

# Area-Preserving Flows-II

- The basic idea of the proof of the theorem is the contruction of an orientation-preserving automorphism homotopic to the identity.

- As a corollary, we get that given M and N any two diffeomorphic surfaces with the same total area, there exists are area-preserving diffeomorphism.
  - This can be constructed explicitly via a PDE.

# Area-Preserving Flows of Minimal Distortion

**Let $M$ and $N$ be two compact surfaces with Riemannian metrics $h$ and $g$ respectively, and let $\phi$ be an area preserving map. This means if $\Omega_g$ and $\Omega_h$ are the area forms then**

$$\phi^*(\Omega_g) = \Omega_h.$$

**Many other area preserving maps from $M \longrightarrow N$ (just compose $\phi$ with any other area preserving map). Which one has the smallest distortion?**

**Minimize the Dirichlet integral with respect to area-preserving maps:**

$$J(\phi) = 1/2 \int_M |D\phi|^2 \ \Omega_h$$

**This leads to explicit gradient descent equations. Method will be discussed when we describe Monge-Kantorovich algorithms.**

# Registration and Mass Transport

**Image registration is the process of establishing a common geometric frame of reference from two or more data sets from the same or different imaging modalities taken at different times.**

**Multimodal registration proceeds in several steps. First, each image or data set to be matched should be individually calibrated, corrected from imaging distortions, cleaned from noise and imaging artifacts. Next, a measure of dissimilarity between the data sets must be established, so we can quantify how close an image is from another after transformations are applied to them. Similarity measures include the proximity of redefined landmarks, the distance between contours, the difference between pixel intensity values. One can extract individual features that to be matched in each data set. Once features have been extracted from each image, they must be paired to each other. Then, a the similarity measure between the paired features is formulated can be formulated as an optimization problem.**

**We can use Monge-Kantorovich for the similarity measure in this procedure.**

# Mass Transportation Problems

- Original transport problem was proposed by Gaspar Monge in 1781, and asks to move a pile of soil or rubble to an excavation with the least amount of work.
- Modern measure-theoretic formulation given by Kantorovich in 1942. Problem is therefore known as *Monge-Kantorovich Problem (MKP).*
- Many problems in various fields can be formulated in term of MKP: statistical physics, functional analysis, astrophysics, reliability theory, quality control, meteorology, transportation, econometrics, expert systems, queuing theory, hybrid systems, and nonlinear control.

# Monge-Kantorovich Mass Transfer Problem

Consider two density functions $\mu_0, \mu_1$ on $\mathbf{R}^d$, such that

$$\int_{\Omega_0} \mu_0 = \int_{\Omega_1} \mu_1.$$

We consider mappings $\tilde{u} : \mathbf{R}^d \to \mathbf{R}^d$ such that for each bounded set $A \subset \mathbf{R}^d$,

$$\int_A \mu_1(x)\, dx = \int_{\tilde{u}(x) \in A} \mu_0\, dx.$$

For $\tilde{u}$ a diffeomorphism we have (***Jacobian equation***)

$$\mu_0(x) = \det(\nabla \tilde{u}(x)) \mu_1 \circ \tilde{u}(x).$$

This the ***mass preservation*** property, and write $\tilde{u} \in MP$. Call such a map ***mass preserving (MP).***

Jacobian equation has many solutions, and we want to pick out an optimal one in some sense. We define the $L^p$***-Kantorovich–Wasserstein*** metric as follows:

$$d_p(\mu_0, \mu_1)^p := \inf_{\tilde{u} \in MP} \int \|\tilde{u}(x) - x\|^p \mu_0(x)\, dx.$$

Optimal MP map, when it exists chooses a map with a preferred geometry (like the Riemann mapping theorem) in the plane.

# Algorithm for Optimal Transport-I

Subdomains with smooth boundaries and positive densities:

$$\Omega_0, \Omega_1 \subset \mathbf{R}^d$$

$$\int_{\Omega_0} \mu_0 = \int_{\Omega_1} \mu_1$$

We consider diffeomorphisms which map one density to the other:

$$\mu_o = \det(D\tilde{u})\mu_1 \circ \tilde{u}$$

We call this the ***mass preservation*** *(MP)* property. We let $u$ be a initial MP mapping.

# Algorithm for Optimal Transport-II

We consider a one-parameter family of MP maps derived as follows:

$$\tilde{u} := u \circ s^{-1},\ s = s(\cdot\,, t),\ \mu_0 = \det(Ds)\mu_0 \circ s$$

Notice that from the MP property of the mapping $s$, and definition of the family,

$$\tilde{u}_t = -\frac{1}{\mu_0} D\tilde{u} \cdot \zeta,\ \zeta = \mu_0\, s_t \circ s^{-1}$$

$$\operatorname{div} \zeta = 0$$

# Algorithm for Optimal Transport-III

We consider a functional of the following form which we infimize with respect to the maps $\tilde{u}$ :

$$M(t) = \int_{\Omega_0} \Phi(\tilde{u}(x,t) - x)\mu_0(x)\ dx$$

$$= \int \Phi(u(y) - s(y,t))\mu_0(y)\ dy,\ \ x = s(y,t),\ \ s^*(\mu_0(x)dx) = \mu_0(y)dy$$

Taking the first variation:

$$M'(t) = -\int \langle \Phi'(u-s),\ \ s_t \rangle \mu_0 dy$$

$$= -\int \langle \Phi'(\tilde{u}(x,t) - x),\ \ \mu_0 s_t \circ s^{-1} \rangle\ \ dx$$

$$= -\int_{\Omega_0} \langle \Phi'(\tilde{u}(x,t) - x),\ \ \zeta \rangle\ \ dx$$

# Algorithm for Optimal Transport-IV

**First Choice:**

$$\zeta = \Phi'(\tilde{u} - x) + \nabla p$$

$$\text{div } \zeta = 0$$

$$\zeta|_{\partial\Omega_0} \text{ tangential to } \partial\Omega_0$$

**This leads to following system of equations:**

$$\tilde{u}_t = -1/\mu_0 D\tilde{u} \cdot (\Phi'(\tilde{u} - x) + \nabla p)$$

$$\Delta p + \text{div } (\Phi'(\tilde{u} - x)) = 0, \text{ on } \Omega_0$$

$$\frac{\partial p}{\partial \vec{n}} + \vec{n} \cdot \Phi'(\tilde{u} - x) = 0, \text{ on } \partial\Omega_0$$

# Algorithm for Optimal Transport-V

This equation can be written in the *non-local* form:

$$\frac{\partial \tilde{u}}{\partial t} = -\frac{1}{\mu_0} D\tilde{u} \cdot (I - \nabla \Delta^{-1} \nabla \cdot) \Phi'(\tilde{u} - x)$$

At optimality, it is known that

$$\Phi'(\tilde{u} - x) = \nabla \alpha$$

where $\alpha$ is a function. Notice therefore for an optimal solution, we have that the non-local equation becomes

$$\frac{\partial \tilde{u}}{\partial t} = 0$$

# Solution of L2 M-K and Polar Factorization

For the L2 Monge-Kantorovich problem, we take

$$\Phi(x) = \frac{|x|^2}{2}$$

This leads to the following "non-local" gradient descent equation:

$$\tilde{u}_t = -1/\mu_0 \nabla \tilde{u}(\tilde{u} - \nabla \Delta^{-1} \ \mathrm{div}(\tilde{u}))$$

Notice some of the motivation for this approach. We take:

$$\tilde{u} = u \circ s^{-1} = \nabla w + \chi, \ \ \mathrm{div}(\chi) = 0 \ \ \textbf{Helmholtz decomp.}$$

The idea is to push the fixed initial u around (considered as a vector field) using the 1-parameter family of MP maps s(x,t), in such a manner as to remove the divergence free part. Thus we get that at optimality

$$u = \nabla w \circ s \ \ \textbf{Polar factorization}$$

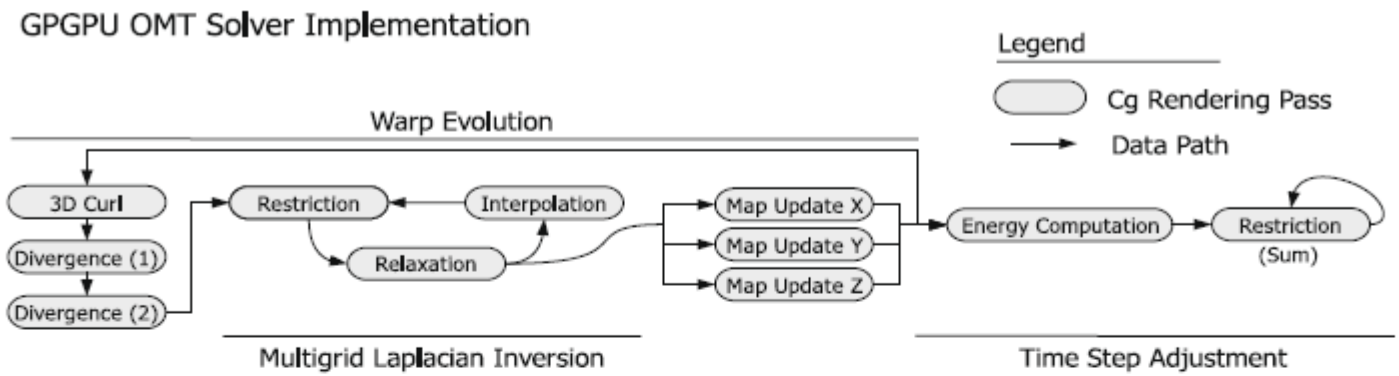


**Fig. 1.** Outline of processing for the OMT solver conducted on the GPU. Processing occurs in two major phases: evolution of the map from source to target volumes and time step adjustment. Each gray rectangle represents one Cg kernel executed on the GPU. Arrows indicate the flow of data volumes through the Cg kernels. The entire process in the figure, above is repeated left to right until convergence.

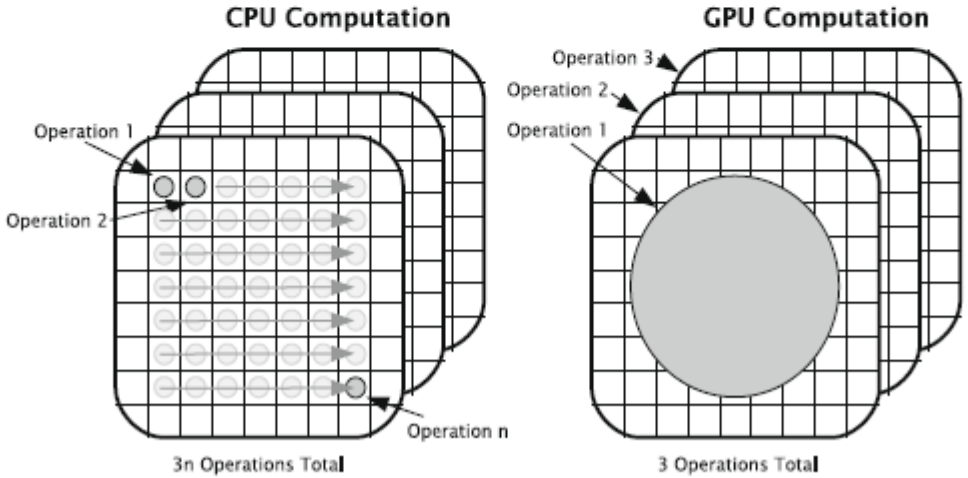


**Fig. 2.** CPU versus GPU solution of PDEs: While the CPU computes updates on data grids one element at a time, the GPU is capable of updating entire grids in one pass due to their massively parallel architecture.

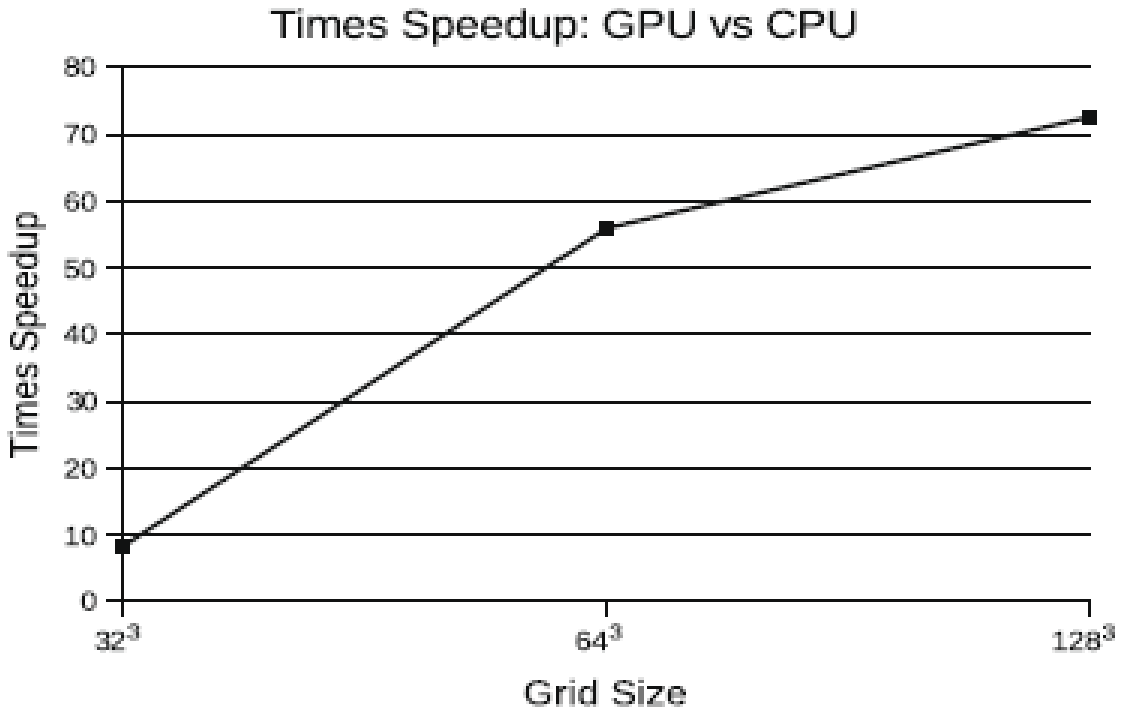


Fig. 3. The GPU realizes an increasing advantage in solving the OMT problem over the CPU as grid size increases up to $128^3$ sized grids.

# Brain Sag

# Beating Heart

# Flame Motion

# Surface Warping-I

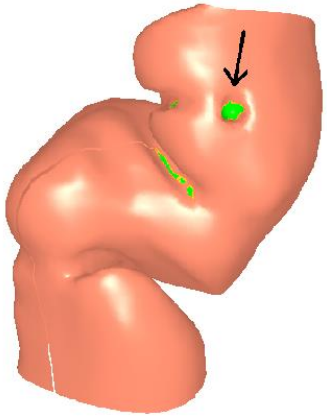

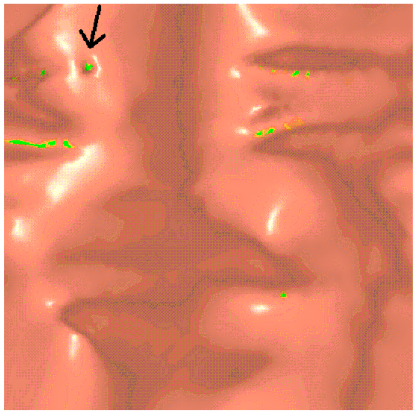

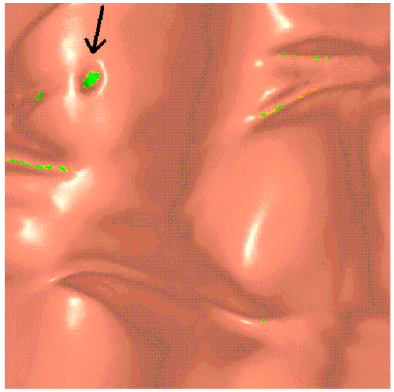

M-K allows one to find area-correcting flattening. After conformally flattening surface, define density mu_0 to be determinant of Jacobian of inverse of flattening map, and mu_1 to be constant. MK optimal map is then area-correcting.

# Surface Warping-II

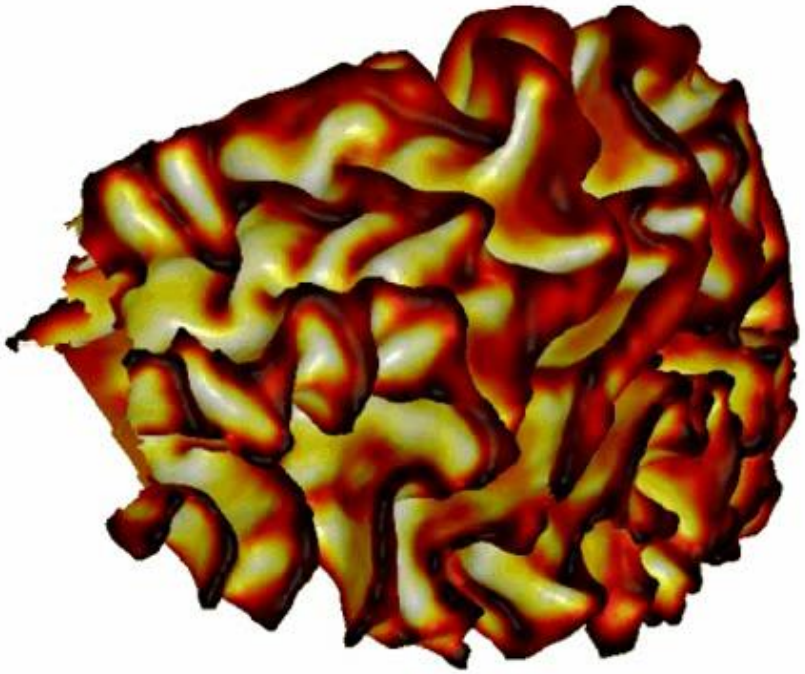

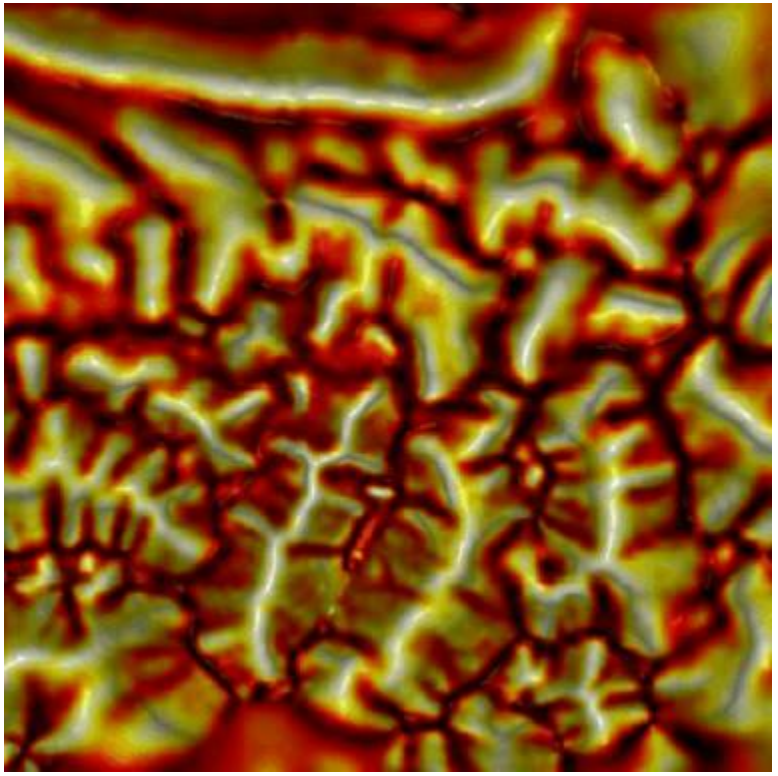

# Example of OMT Mapping on Spherical Shape

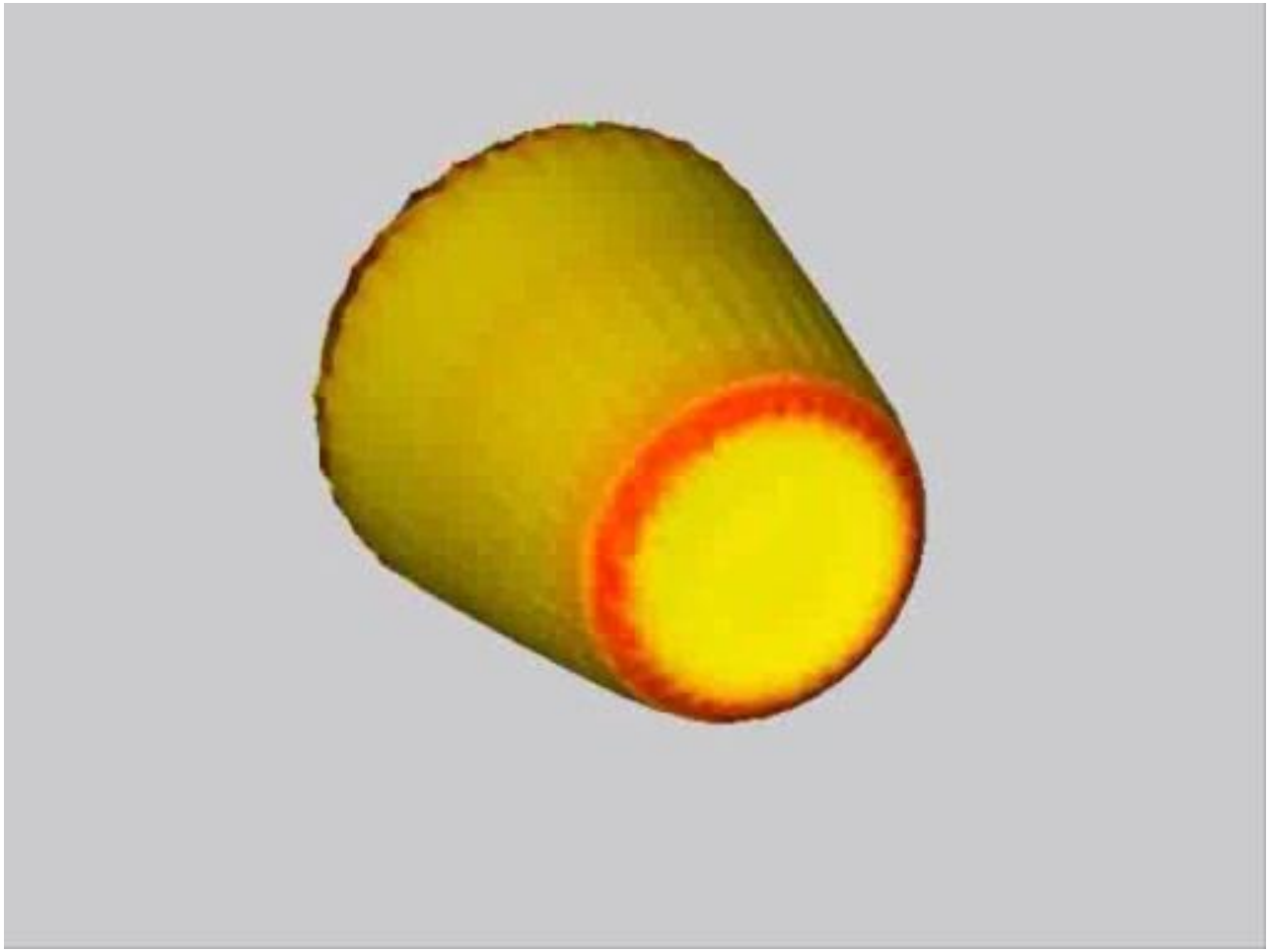

# Hexahedral Meshes-I

Hexahedral vs. tetrahedral meshes

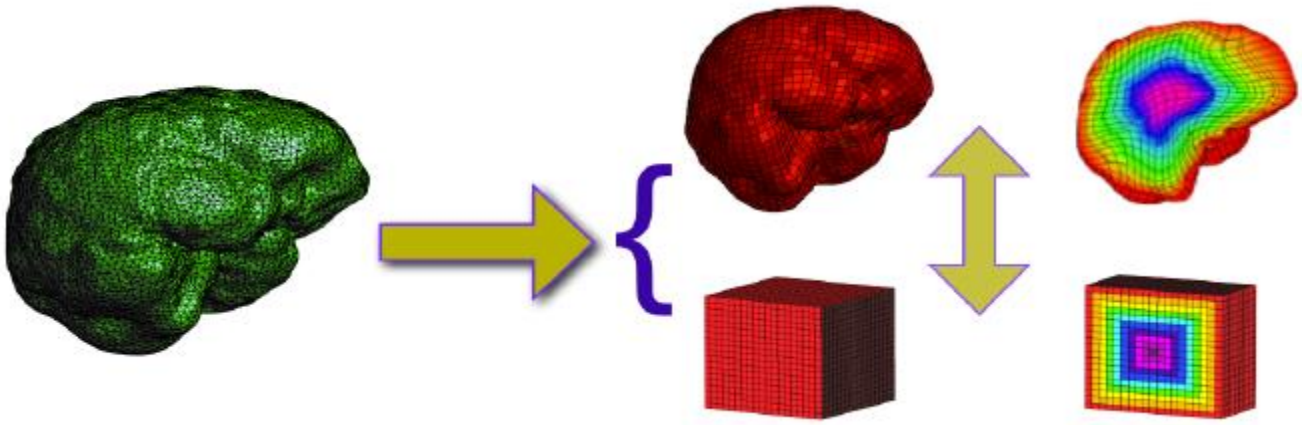

Construct a volume preserving mapping onto a solid cube and generate canonical hexahedral (as opposed to tetrahedral)

Idea: first register to a cube, generate mesh, then deform to preserve volume

# Hexahedral Meshes-II

Volumetric results for a database of 3-D prostates extracted from MRI imaging

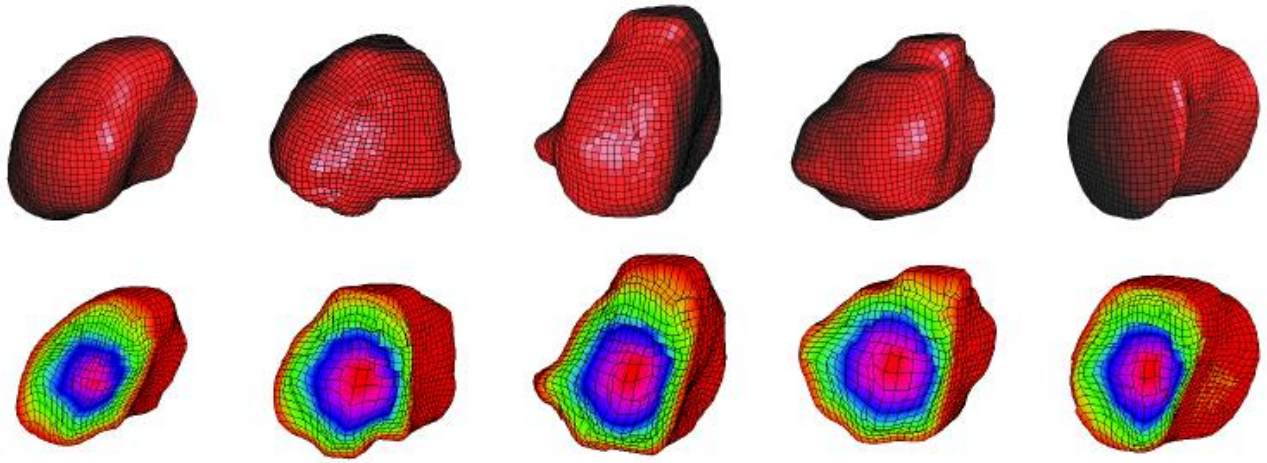

Top row: prostates
Bottom row: volumetric map shown via mesh slicing
(shell color --- layer of cube)

# OMT for Cardiac Dynamics

Afib is joint work with Rob Macleod (Utah)

# Atrial Fibrillation Video

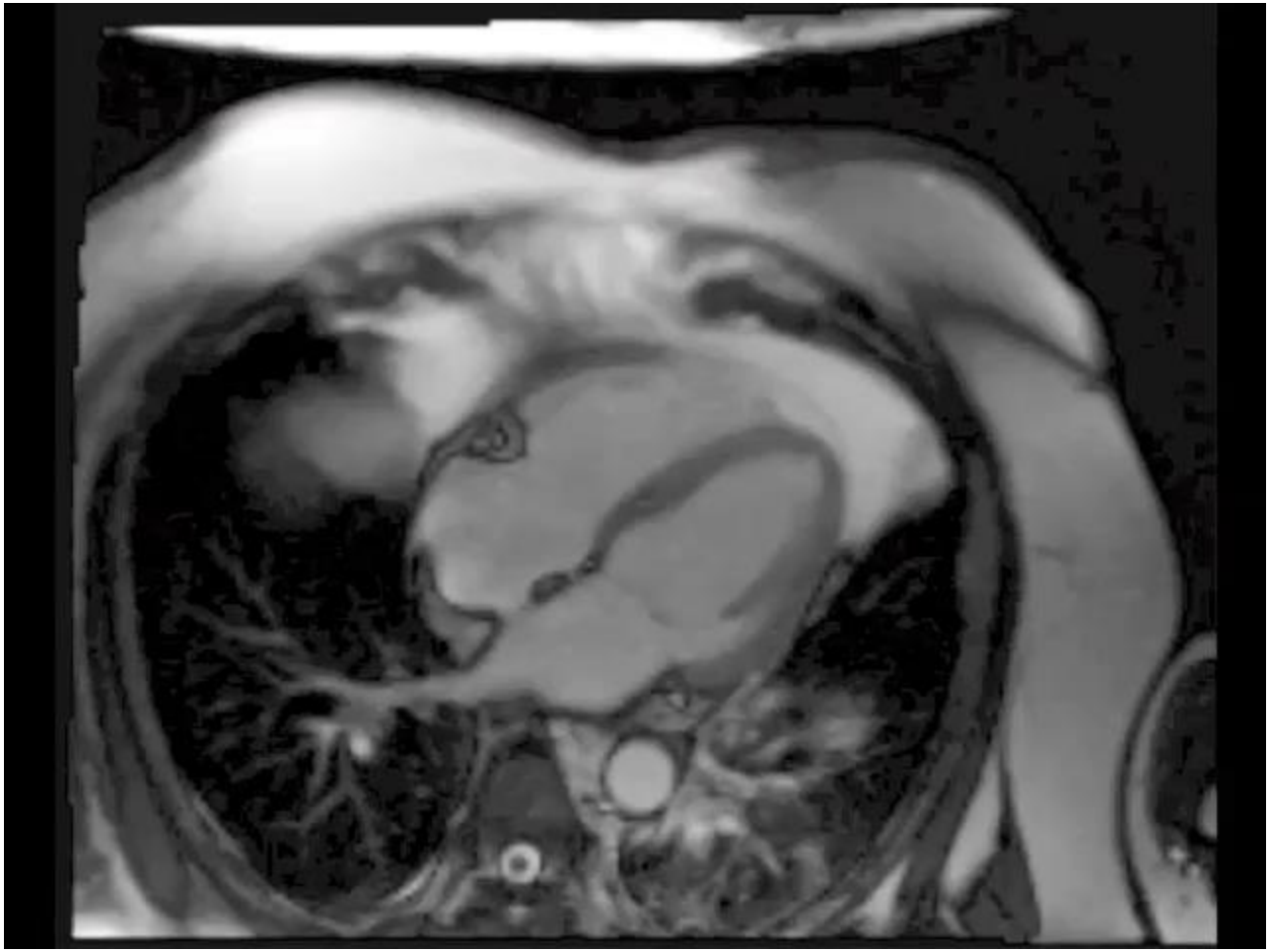

# What We Know About AF

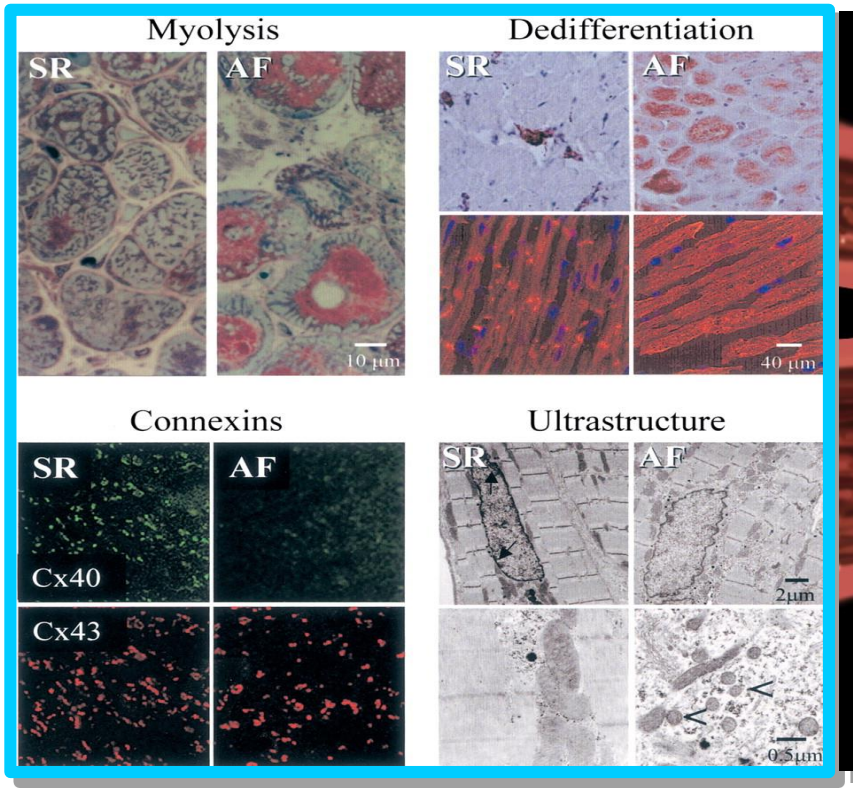


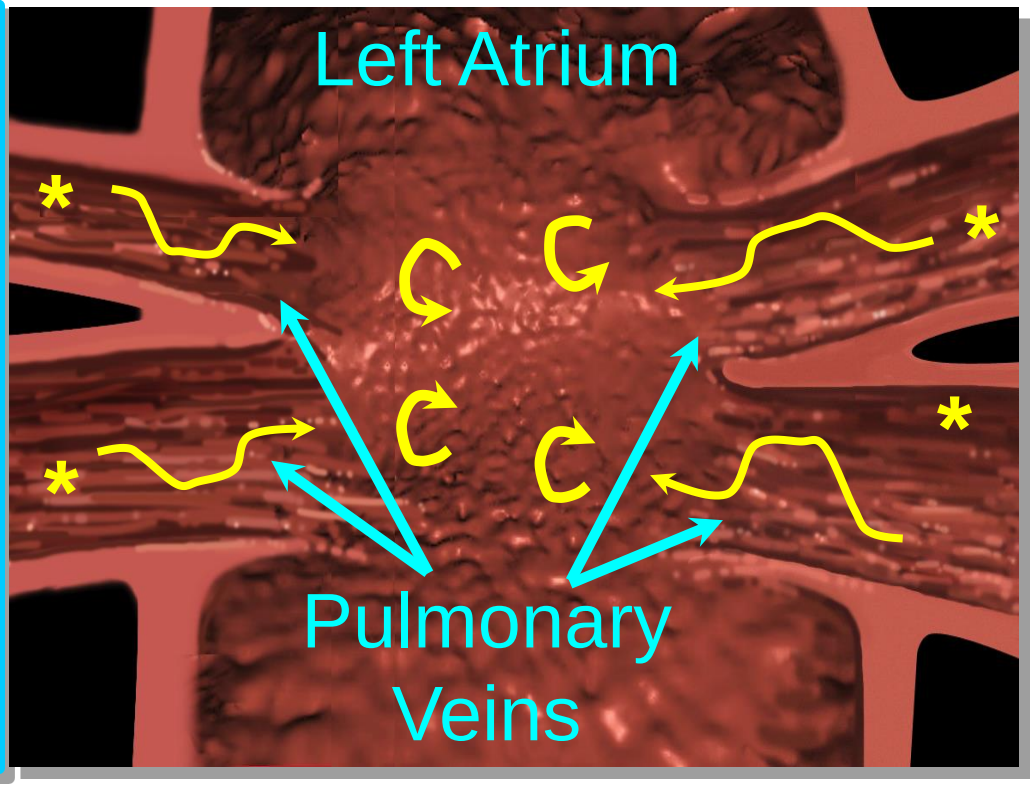


Substrate

Triggers

# The Million $ Mechanistic Question

Afib begets Afib

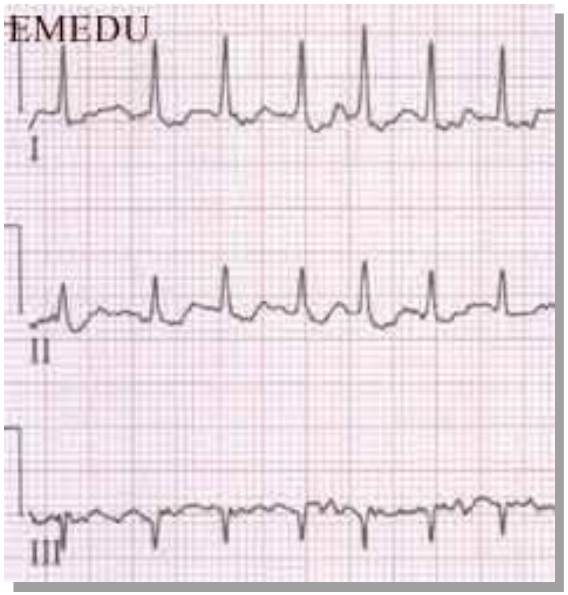


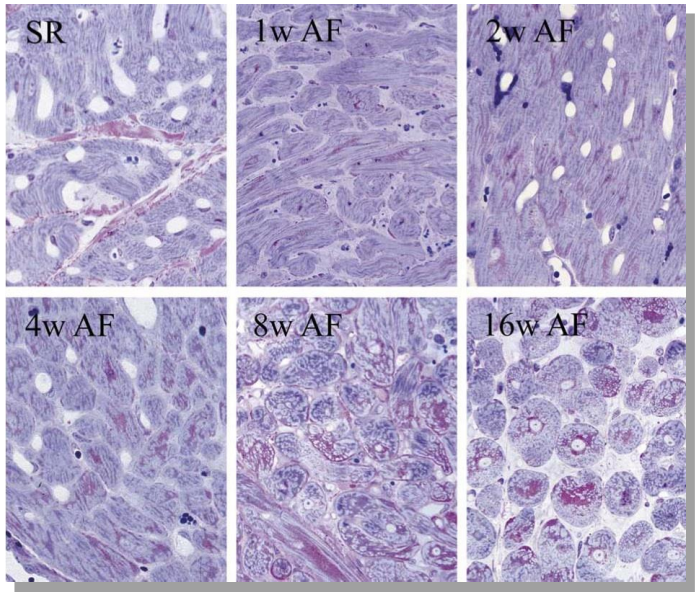


Afib is a tissue disease

# Longitudinal Interpolation of Image and Shape

Two images scanned at $t = T_0$ and $t = T_1 (> T_0)$
Generate image samples at times $t \in [T_0, T_1]$
via ***OMT-transport-interpolation*** between samples

Starting at:

$\mu_0 := I(\boldsymbol{x}, T_0)/\|I(T_0)\|_2$ and $\mu_1 := I(\boldsymbol{x}, T_1)/\|I(T_1)\|_2$

optimal transport mapping $\tilde{\boldsymbol{u}}$ computed
by minimizing the Kantorovich-Wasserstein functional equation

## Specifics

Set $\boldsymbol{v} := (\tilde{\boldsymbol{u}}(\boldsymbol{x}) - \boldsymbol{x})/(T_1 - T_0)$
define $\boldsymbol{w} : \mathbb{R}^d \times [T_0, T_1] \to \mathbb{R}^d$ as

$$\boldsymbol{w}(\boldsymbol{x}, t) := \boldsymbol{x} + (t - T_0)\boldsymbol{v} \tag{1}$$

define the image sequence:

$$I(\boldsymbol{x}, t) := \det\left(J(\boldsymbol{w}(\boldsymbol{x}, t))\right) \mu_0(\boldsymbol{w}(\boldsymbol{x}, t)) \tag{2}$$

Note that

$$I(\boldsymbol{x}, t)|_{t=T_0} = \mu_0(\boldsymbol{x}) \quad \text{and} \quad I(\boldsymbol{x}, t)|_{t=T_1} = \mu_1(\boldsymbol{x}) \tag{3}$$

This is a ***geodesic path*** in the space of densities with respect to the Wasserstein 2-metric. The Wasserstein metric imparts a natural Riemannian structure to the space of densities.

## Image flow-extrapolation

Geodesics can be extrapolated (slightly) into the future

– let $t$ go beyond $T_1$ and obtain an estimated density at time beyond $T_1$
– since $\boldsymbol{u}$ is diffeomorphism, so is $\boldsymbol{w}$ for all $t \in [T_0, T_1]$
– for $t > T_1$, $\boldsymbol{w}$ exists and is diffeomorphic for $t \in [T_0, T_1 + \epsilon]$.

## Interpolation of images/statistics

The image $I(\boldsymbol{x})$ above can also be a binary volume representation of an anatomical shape. Statistical shape analysis can then be "interpolated" to any time point between $T_0$ and $T_1$.

Denote shapes at times $T_0$ and $T_1$ as:
$\check{I}_1^A(\boldsymbol{x}, T_0), \ldots, \check{I}_M^A(\boldsymbol{x}, T_0)$ and $\check{I}_1^A(\boldsymbol{x}, T_1), \ldots, \check{I}_M^A(\boldsymbol{x}, T_1) : \mathbb{R}^3 \longrightarrow \{0, 1\}$

Denote a second group of shapes as:
$\check{I}_1^B(\boldsymbol{x}, T_0), \ldots, \check{I}_N^B(\boldsymbol{x}, T_0)$ and $\check{I}_1^B(\boldsymbol{x}, T_1), \ldots, \check{I}_N^B(\boldsymbol{x}, T_1) : \mathbb{R}^3 \longrightarrow \{0, 1\}$

Using OMT, a continuous shape trajectory between $T_0$ and $T_1$ can be computed as $\check{I}_i^j : \mathbb{R}^3 \times [T_0, T_1] \longrightarrow [0, 1]$

# Registration

Then, at time $t \in [T_0, T_1]$, in order to compute the regions where the two groups are statistically different, we first **register** the two groups $\check{I}_1^A(\boldsymbol{x}, t), \ldots, \check{I}_M^A(\boldsymbol{x}, t)$ and $\check{I}_1^B(\boldsymbol{x}, t), \ldots, \check{I}_N^B(\boldsymbol{x}, t)$.

Registration is accomplished by arbitrarily picking one of the shapes, $\check{I}$, and registering all the others to it by minimizing the energy $E(\mathcal{A}_i^j)$ with respect to each similarity transformation $\mathcal{A}_i^j : \mathbb{R}^3 \longrightarrow \mathbb{R}^3$, where

$$E(\mathcal{A}_i^j) := \int_\Omega \left( \check{I}_i^j(\mathcal{A}_i^j \circ \boldsymbol{x}, t) - \check{I}(\boldsymbol{x}, t) \right)^2 \mathrm{d}\boldsymbol{x}, \quad j \in \{A, B\}, \tag{4}$$

$$i \in \{1, \ldots, M \text{ or } N\}. \tag{5}$$

After registration, we denote the registered shapes: $I_1^A(\boldsymbol{x}, t), \ldots, I_M^A(\boldsymbol{x}, t)$ and $I_1^B(\boldsymbol{x}, t), \ldots, I_N^B(\boldsymbol{x}, t)$.

# Mean Shape

– The mean shape $M : \mathbb{R}^3 \times [T_0, T_1] \rightarrow [0, 1]$ is the arithmetic average:

$$M(\boldsymbol{x}, t) = \frac{1}{M+N}\left(I_1^A(\boldsymbol{x}, t) + \cdots + I_M^A(\boldsymbol{x}, t) + I_1^B(\boldsymbol{x}, t) + \cdots + I_N^B(\boldsymbol{x}, t)\right)$$

– The mean shape surface $S(t) \subset \mathbb{R}^3$ is the 0.5-isosurface of $M(\boldsymbol{x}, t)$

– For each of the registered shapes, $I_i^j$'s,
a signed distance function $D_i^j : \mathbb{R}^3 \times [T_0, T_1] \rightarrow \mathbb{R}$ is:

$$D_i^j(\boldsymbol{x}, t) = \begin{cases} \inf_{\boldsymbol{y} \in S} \|\boldsymbol{x} - \boldsymbol{y}\|_2, & \text{if } I_i^j(\boldsymbol{x}, t) \leq 0.5 \\ -\inf_{\boldsymbol{y} \in S} \|\boldsymbol{x} - \boldsymbol{y}\|_2, & \text{if } I_i^j(\boldsymbol{x}, t) > 0.5 \end{cases}$$

$$j \in \{A, B\},\ i \in \{1, \ldots, M \text{ or } N\}$$

# Hypothesis Testing

All shapes are converted to functions defined on the same domain $S$ by restricting $D_i^j$'s to $S$

For each $s$ on $S$, two groups of numbers $\{D_i^A(s)\}$ and $\{D_i^B(s)\}$ can be extracted. Under the ***null hypothesis*** that the means of the two groups are the same, we perform the student $t$-test, and the corresponding $p$-value is recorded for the point $s$

The final corrected $p$-values give a scalar $p$-value map $P : S \rightarrow [0, 1]$ defined on the mean shape surface at each time

# Longitudinal shape analysis

- Two groups of LA shapes
  - AFib cured/recurred after ablation
  - Each subject has two time points
- Shape differences along time?
  - Shape interpolation using optimal mass transport
  - Shape analysis at continuous time points
  - Statistical differences in the distribution of the contrast agent (related with fibrosis) between cured/recurred groups?

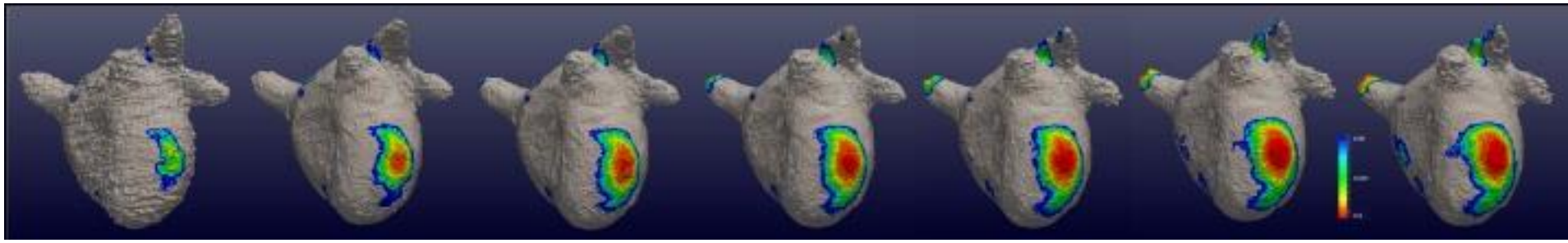

# Traumatic Brain Injury

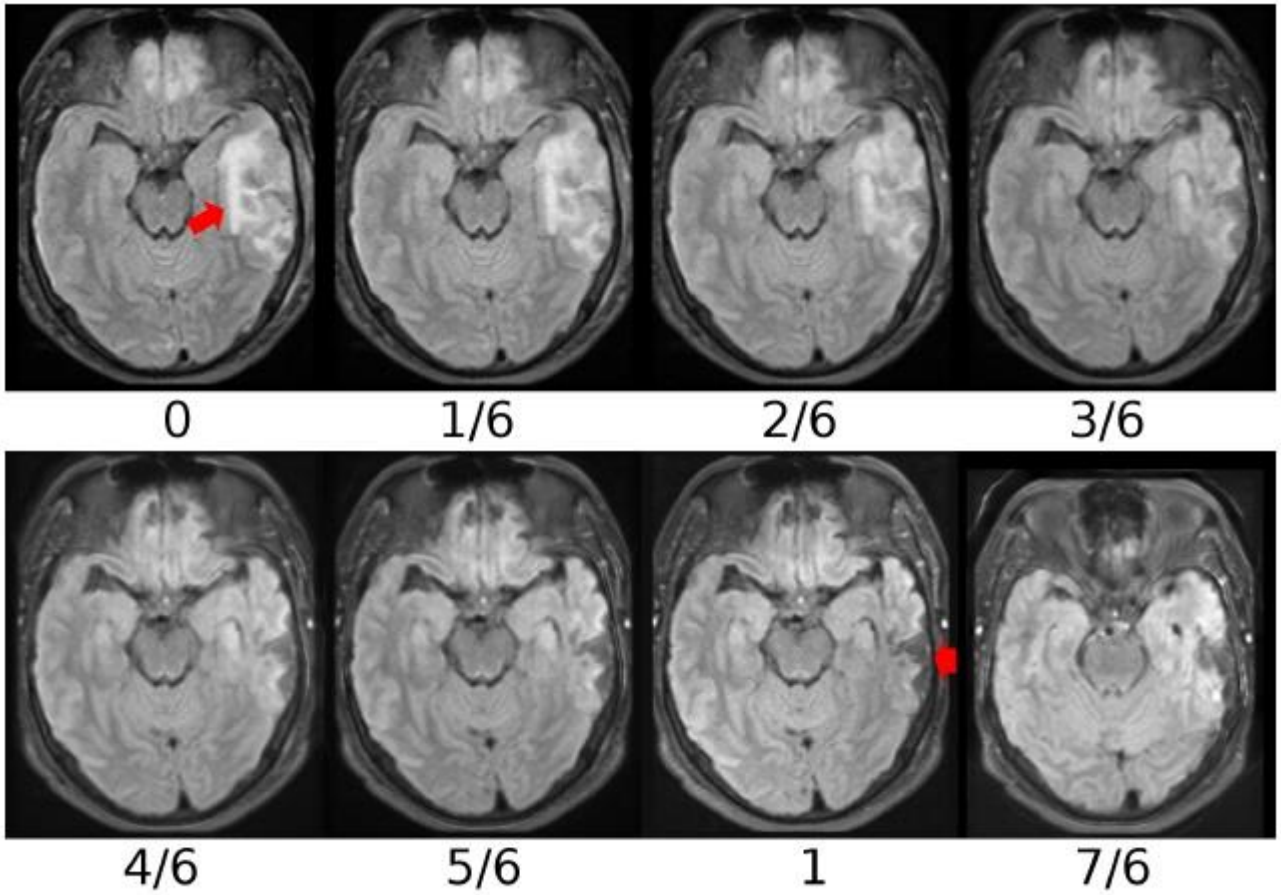


Healing of TBI. The number below each image indicates "time." Only times 0 and 1 are real images, and all the others are computed using the proposed OMT method. The healing process of the injured region pointed to the arrow is better illustrated by the gradual progression than simply having the two original images at time 0 and 1. The prediction in the near future is shown on the bottom-right.

# Species Classification

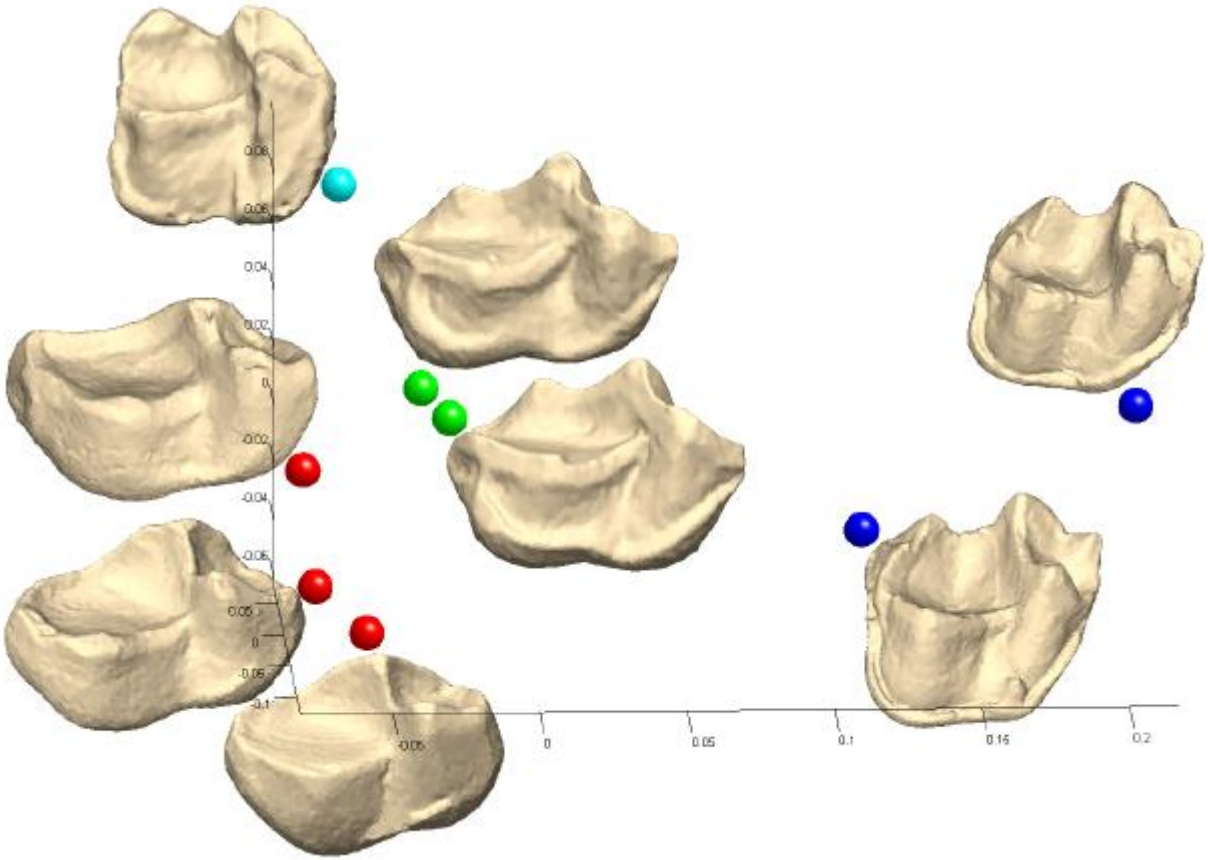

Embedding of the distance graph of eight teeth models using multi-dimensional scaling. Different colors represent different lemur species. The graph suggests that the geometry of the teeth might be used to classify species. Taken from CONFORMAL WASSERSTEIN DISTANCES: COMPARING SURFACES IN POLYNOMIAL TIME by Lipman and Daubechies.

# Matrix OMT - motivation

Optimal power transport (OPT)
– antenna arrays
– time-series analysis
– spectrograms

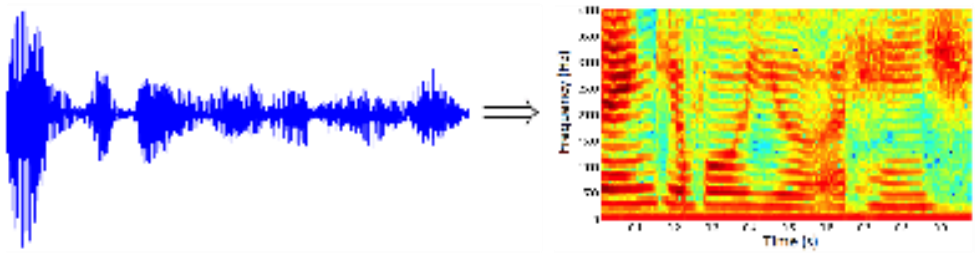

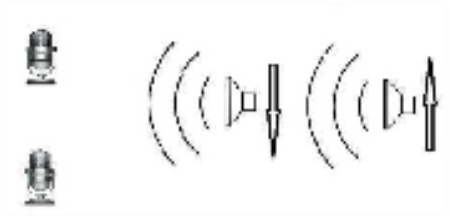

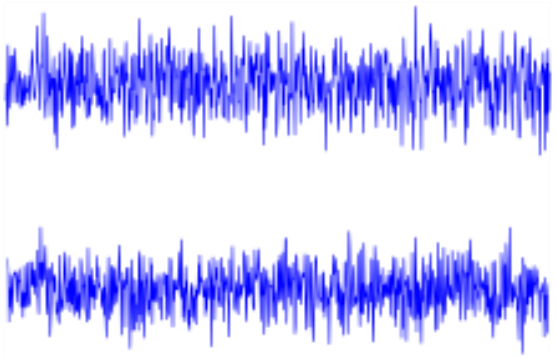

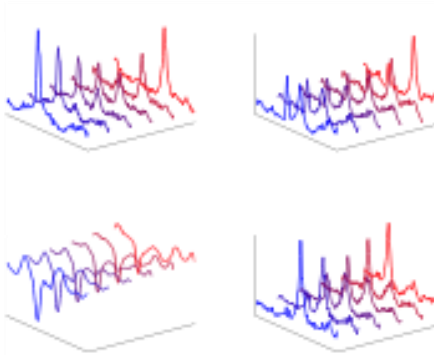

# Matrix OMT formulation

$\mathcal{M}_0, \mathcal{M}_1$ matrix densities on $\mathbb{C}^n$ — Hermitian in $[0,\ 1] \times \mathbb{C}^{n \times n}$

Joint density $\mathcal{M}$ on $\mathbb{C}^n \otimes \mathbb{C}^n$ — in $[0,\ 1] \times \mathbb{C}^{n^2 \times n^2}$

$$\mathrm{trace}_0(\mathcal{M}) = \mathcal{M}_1,\ \mathrm{trace}_1(\mathcal{M}) = \mathcal{M}_0$$

$$C(x,y) = \underbrace{\|x-y\|^2}_{\text{transp. cost}} + \lambda \underbrace{\|\underline{\mathrm{tr}_1}(\mathcal{M}) - \underline{\mathrm{tr}_0}(\mathcal{M})\|_{\mathrm{F}}^2}_{\text{“rotation" cost}}$$

where $\underline{\mathrm{tr}_i}\mathcal{M} := \frac{\mathrm{tr}_i \mathcal{M}}{\mathrm{tr}\,\mathcal{M}}$

$$\min_{\mathcal{M}} \int_{X \times Y} \Big( \underbrace{\|x-y\|^2 + \lambda \|\underline{\mathrm{tr}_1}(\mathcal{M}) - \underline{\mathrm{tr}_0}(\mathcal{M})\|_{\mathrm{F}}^2}_{C(x,y)} \Big)\, \mathrm{tr}(\mathcal{M}) dx dy$$

$\Rightarrow$ convex optimization problem

# Matrix-valued spectrogram

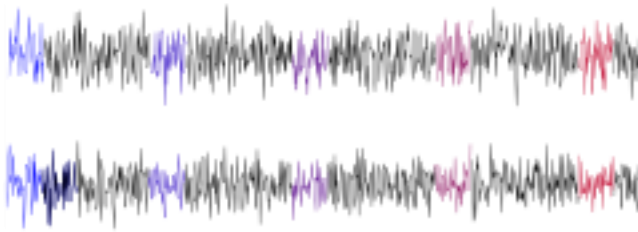

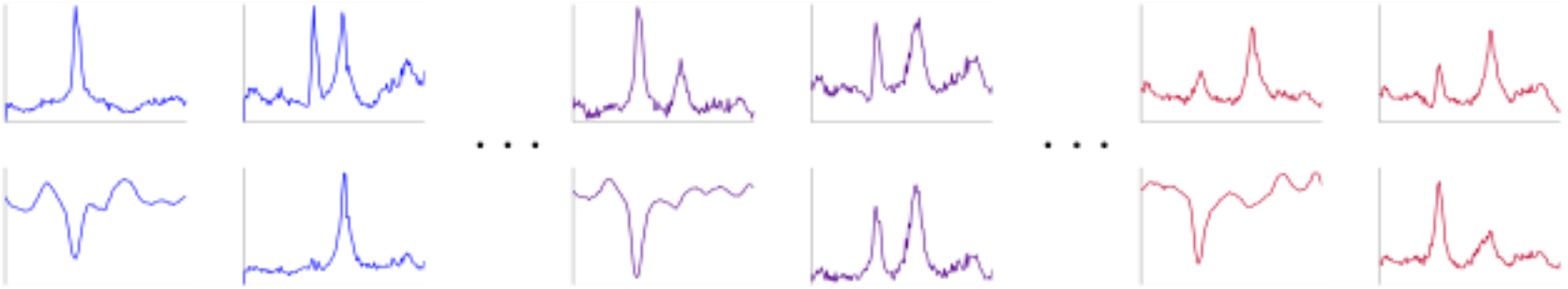

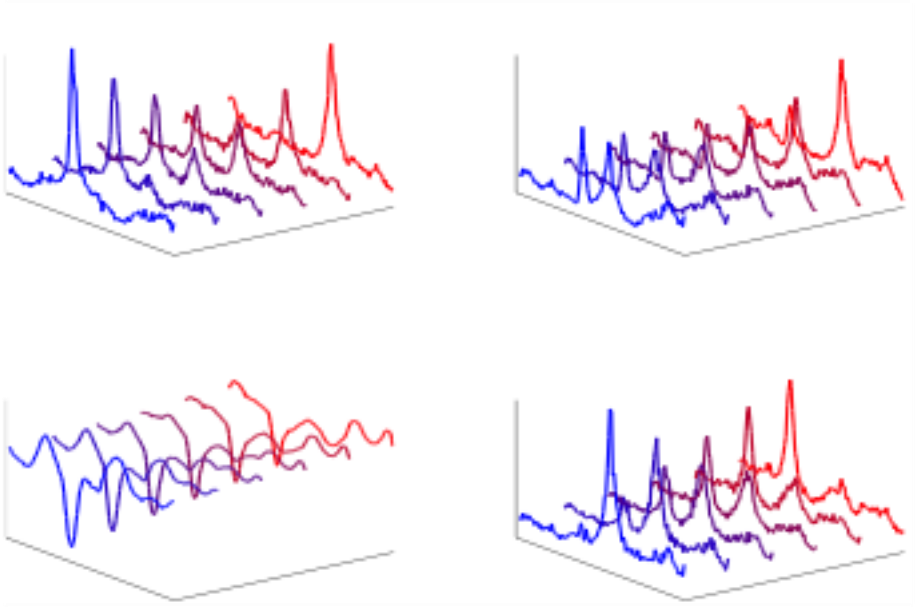

# Geodesic tracking

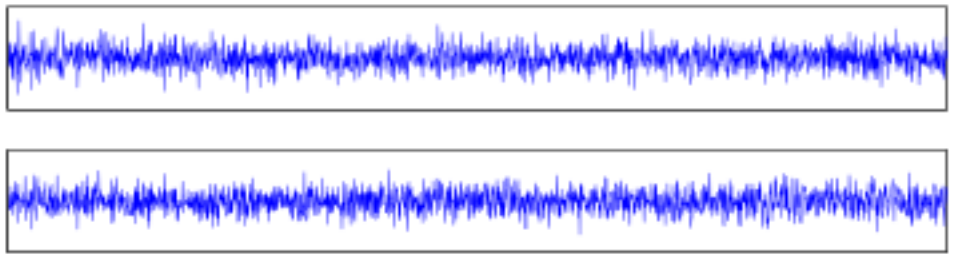

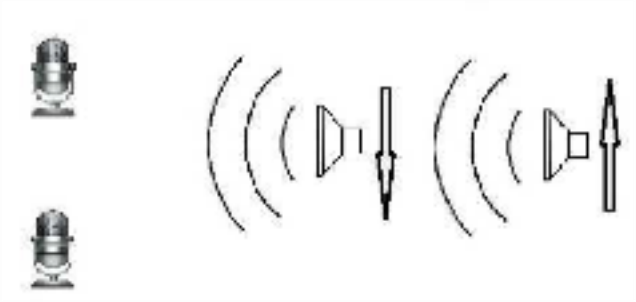

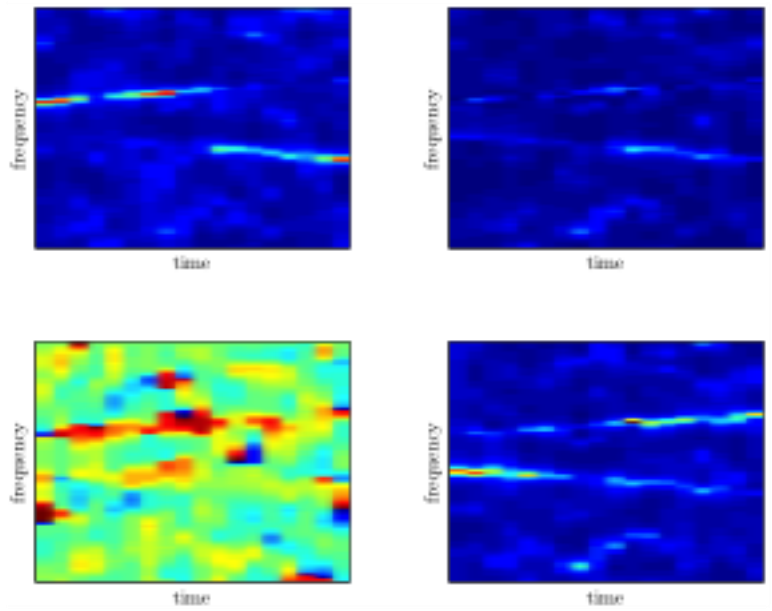


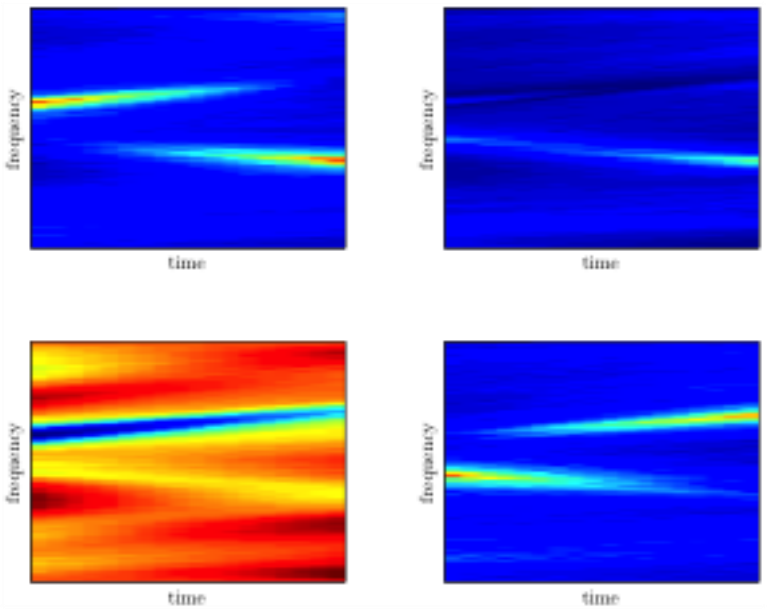


*"Maximum-entropy" spectrogram*

*OMT interpolation of $\mathcal{M}_t$'s*

# Geodesic tracking

– eigenvectors at “peak” frequencies $\sim$ directionality of source

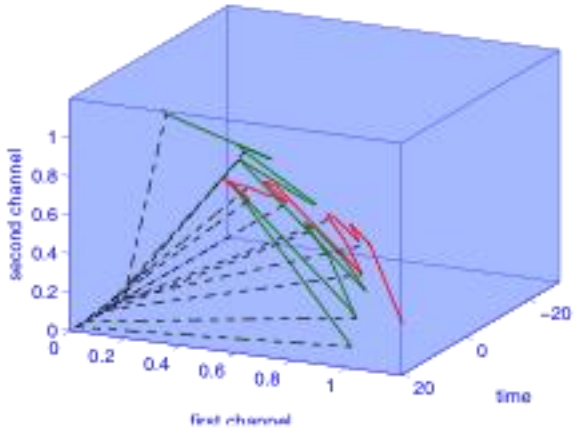


*Maximum-entropy spectrogram*

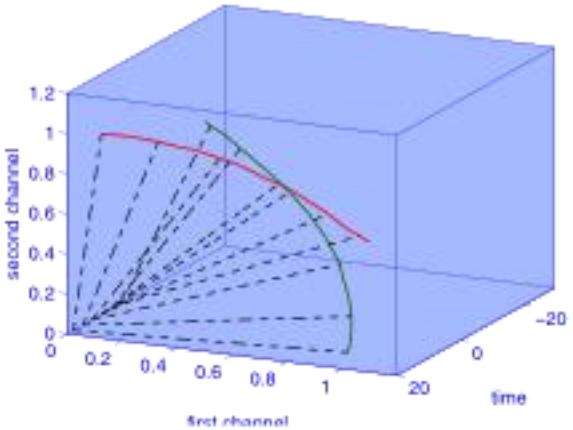


*OMT tracking*

# Concluding Remarks

- Segmentation
  - Dynamic Active Contours
  - Finsler Geometry
  - Bayesian Statistics (Particle Filtering)
  - Interactive Control Methods

- Registration
  - Optimal Mass Transport
  - Texture Mappings
  - Meshes